JOURNAL OF GEOPHYSICAL RESEARCH, VOL. 112, D02205, doi:10.1029/2005JD007024, 2007

Global impacts of aerosols from particular source regions and sectors

Dorothy Koch,[1] Tami C. Bond,[2] David Streets,[3] Nadine Unger,[1,4] and Guido R. van der Werf[5]

Received 22 December 2005; revised 12 September 2006; accepted 25 September 2006; published 24 January 2007.

[1] We study the impacts of present-day aerosols emitted from particular regions and from particular sectors, as predicted by the Goddard Institute for Space Studies GCM. We track the distribution and direct radiative forcing of aerosols, including sulfate and black and organic carbon, emitted from major source regions (North America, Europe, south Asia, Southeast Asia, South America, and Africa). We also partition the emissions by sector, including industrial, power, residential, transport, biomass burning, and natural. Southeast Asia produces 15% and 10% of the world's black carbon and sulfate and exports over 2/3 of this burden over the Northern Hemisphere. About 1/2 of the SO_2 emitted by Southeast Asia and Europe is not converted to sulfate because of oxidant limitation. Although Africa has the largest biomass burning emissions, South America generates a larger (about 20% of the global carbonaceous) aerosol burden; about 1/2 of this burden is exported and dominates the carbonaceous aerosol load in the Southern Hemisphere. Calculated direct anthropogenic radiative forcings are -0.29, -0.06, and 0.24 W m^{-2} for sulfate, organic, and black carbon, respectively. The largest BC radiative forcings are from residential (0.09 W m^{-2}) and transport (0.06 W m^{-2}) sectors, making these potential targets to counter global warming. However, scattering components within these sectors reduce these to 0.04 and 0.03 W m^{-2}, respectively. Most anthropogenic sulfate comes from power and industry sectors, and these sectors are responsible for the large negative aerosol forcings over the central Northern Hemisphere.

Citation: Koch, D., T. C. Bond, D. Streets, N. Unger, and G. R. van der Werf (2007), Global impacts of aerosols from particular source regions and sectors, *J. Geophys. Res.*, *112*, D02205, doi:10.1029/2005JD007024.

1. Introduction

[2] Aerosols are thought to have important impacts on climate and health, although the magnitudes of these impacts remain quite uncertain. While source estimates are generally becoming more thorough, ongoing challenges in these estimates result from lack of knowledge about human behavior and technology. The chemical evolution of aerosol particles and the inhomogeneity of aerosol global distributions further confound estimates of their concentrations and impacts. Furthermore, their impacts on climate are complex and difficult to quantify and to observe. In this study we seek new insight into aerosol sources, distributions and impacts by tracking the aerosols according to their region of origin, sector of origin and chemical composition.

[3] Some aerosols are generated naturally, some result from fossil fuel combustion and others by both natural and anthropogenic burning of vegetation. Once produced, the particles are removed from the troposphere relatively quickly (within a few days), primarily by precipitation scavenging. As a result, their distribution is very inhomogeneous, both in the horizontal and vertical directions.

[4] Anthropogenic aerosols are believed to affect climate in several ways. They primarily scatter and cool the Earth's surface. However if dark and absorbing components are present they also may heat the air in which they are suspended. To the extent that particle number has increased, clouds are believed to be brighter and longer-lived (indirect effect [*Andreae*, 1995; *Twomey*, 1997; *Albrecht*, 1989]). Black carbon (BC), which is dark and absorbing, may perturb the vertical thermal gradient and hence alter the level and degree of cloud formation [*Hansen et al.*, 1997]. If BC deposits on ice/snow it may lower the ice or snow albedo and promote melting [*Hansen and Nazarenko*, 2004].

[5] Thus the various climate impacts and the challenges of formulating model aerosol parameterizations have made aerosols among the most uncertain elements in climate research. Numerous modeling studies have looked at the transport and climate impacts of aerosols. Some include

[1]NASA Goddard Institute for Space Studies, Columbia University, New York, New York, USA.
[2]Department of Civil and Environmental Engineering, University of Illinois, Urbana-Champaign, Urbana, Illinois, USA.
[3]Argonne National Laboratory, Argonne, Illinois, USA.
[4]Now at Rubenstein School of Environment and Natural Resources, University of Vermont, Burlington, Vermont, USA.
[5]Department of Hydrology and Geo-Environmental Sciences, Vrije Universiteit, Amsterdam, Netherlands.

0148-0227/07/2005JD007024$09.00

single chemical components (sulfate, black carbon or BC, organic carbon or OC, dust, sea salt [e.g., *Roberts and Jones*, 2004; *Chung and Seinfeld*, 2005; *Wang*, 2004; *Miller et al.*, 2006; *Grini et al.*, 2005; *Berglen et al.*, 2004; *Bell et al.*, 2005]). More recently, multicomponent global aerosol models have been developed (*Textor et al.* [2006] summarize, evaluate and compare current multicomponent global aerosol models). Some include direct radiative effects [e.g., *Koch and Hansen*, 2005; *Koch et al.*, 2006; *Reddy et al.*, 2005a, 2005b; *Takemura et al.*, 2002] and indirect effects (*Lohmann and Feichter* [2005] summarize recent model results). These generally consider the anthropogenic effects on climate due to one or all major chemical species.

[6] However, it becomes increasingly important to understand how actions in particular regions impact air quality and climate. We may also want to evaluate possible benefits of reducing emissions. These require a new perspective, one that links actions and sources within regions to their impacts on air quality and global climate. This may be done within a model by isolating source regions and/or sectors, and few studies have taken such an approach. *Reddy et al.* [2005b] consider the direct forcing effects due to biomass burning, fossil fuel and natural sources. *Jacobson* [2002] compared the climate impacts of diesel and gasoline emission fractions of the transport sector, demonstrating a significant warming impact from BC in diesel. *Rasch et al.* [2000] modeled the fate of SO_2 emitted from particular regions (Europe, North America, Asia and rest-of-the-world or ROW). They showed that ROW SO_2 is more likely to be oxidized than SO_2 from the industrial regions and that SO_2 emitted from Asia is most prone to long-range transport. *Koch and Hansen* [2005] modeled the BC emitted from some regions (Europe, North America, north Asia, Southeast Asia), and demonstrated that the largest portion of Arctic BC is derived from (south-southeast) Asia.

[7] The goal of this study is to track aerosols emitted from particular regions and particular sectors and to estimate their impacts on global aerosol pollution and energy balance. This study follows up on *Koch and Hansen* [2005], which focused primarily on source regions of Arctic BC. Here we consider 3 species: sulfate, organic carbon and black carbon. Our choice of regions of origin also differ, now we divide the ''Southeast Asia'' region of *Koch and Hansen* [2005] into south Asia (roughly India) and Southeast Asia (roughly China). As we will show, these two regions differ greatly in their source types and impacts. We also consider the importance of the largest biomass burning source regions, South America and Africa. Thus our goal is to consider the degree and mode of export from some of the largest aerosol source regions.

[8] Various regions differ in the composition of emitted aerosols, because of their local sectoral sources. Thus, for example, the industry and power sectors are particularly important in North America and Europe and also produce large amounts of SO_2 (precursor to sulfate). Asia has relatively greater residential sector emissions and therefore larger carbonaceous aerosol emissions. In order to discern the importance and spatial distribution of various sectors, we divide and track our emissions (of OC, BC and sulfate) in the following sectoral categories: transport, residential, power, industrial, open biomass burning and natural. This enables investigation of the possible impacts of changing emissions within particular sectors. We also consider the extent to which model-derived quantities such as burden and forcing are proportional to emissions; that is, can we infer aerosol impacts using emissions estimates alone?

2. Model Description

[9] We use the GISS ModelE aerosol simulation, described in detail by *Koch et al.* [2006] and *Koch and Hansen* [2005]. The aerosol simulation code is embedded in the GISS ModelE general circulation model [*Schmidt et al.*, 2006]. Model vertical resolution is 20 sigma-pressure levels, average midpoint values are 974, 949, 909, 847, 760, 630, 470, 337, 247, 180, 130, 95, 67, 45, 27, 15, 6.5, 2, 0.65 and 0.2 mbar. Horizontal resolution is $4^\circ \times 5^\circ$. Tracer mass, humidity and heat are transported using the quadratic upstream scheme. Tracer dry deposition uses a resistance-in-series scheme; settling of aerosols is included. Model cloud types are convective and stratiform, including a prognostic treatment of stratiform cloud water [*Del Genio et al.*, 1996, 2005; *Schmidt et al.*, 2006]. Wet chemistry and deposition of soluble species are tightly coupled to the GISS model cloud schemes, so that dissolution and aqueous chemistry follow cloud condensation, species are transported, entrained and detrained with cloud water, rainout is determined by autoconversion, below cloud scavenging depends upon precipitation amount, and release from the cloud or from falling rain depends upon cloud or rain evaporation.

[10] The model aerosols interact with radiation and are assumed to be externally mixed. The aerosol optical thickness and radiative forcing calculations are based on Mie code embedded in the GCM [*Schmidt et al.*, 2006]. Effective radii (dry) are assumed to be 0.2, 0.3 and 0.1 μm for sulfate, organic carbon (OM) and black carbon (BC), respectively. For BC the real and imaginary parts of the refractive index are 1.56 and 0.5 at 550 nm [*Nilsson*, 1979]. Sulfate and OC optical and radiative parameters (including particle size, density and refractive index) depend on relative humidity, and include formulation for deliquescence [*Tang and Munkelwitz*, 1991, 1994; *Tang*, 1996]. The dependence of effective radius, refractive index (real part) and extinction efficiency for some sample values of relative humidity are given in Table 1. At visible wavelengths, the sulfate imaginary refractive index is sufficiently small to be considered as conservative scattering. Organic carbon refractive indices are similar to those of sulfate, except that OC is slightly absorbing, using the imaginary refractive index given by *Kirchstetter et al.* [2004]. Additional details on optical and radiative schemes are provided by *Koch and Hansen* [2005], *Koch et al.* [2006] and *Schmidt et al.* [2006]. In this study we consider direct (and not indirect) radiative forcing effects. Radiative forcings at top of the atmosphere (TOA) are calculated online instantaneously, taking the difference between the short-wave TOA radiation with and without each aerosol component.

[11] The simulated mass species include sulfate, sulfur dioxide (SO_2), hydrogen peroxide (H_2O_2), dimethylsulfide (DMS), organic matter (OM) and black carbon (BC). Organic matter is assumed to include organic carbon (OC) and associated compounds, such that OM = 1.3 $\times$ OC [*Liousse et al.*, 1996]. Dry and aqueous sulfur chemistry are

Table 1. Optical Properties as Function of RH[a]

RH	25	50	75	85	95	99
			Sulfate			
Radius, μm	0.20	0.24	0.28	0.32	0.42	0.71
Refractive index (real)	1.53	1.44	1.41	1.39	1.36	1.34
Extinction efficiency, $m^2\ g^{-1}$	4.7	6.9	10	13	26	78
			Organic Carbon			
Radius, μm	0.30	0.31	0.32	0.33	0.35	0.38
Refractive index (real)	1.53	1.51	1.50	1.49	1.47	1.44
Extinction efficiency, $m^2\ g^{-1}$	5.0	5.4	5.8	6.2	6.9	8.2

[a]At 550 nm.

described by *Koch et al.* [1999, 2006]. Non-biomass-burning BC and OM are assumed to be emitted as insoluble, aging to soluble with e-fold lifetimes of 1 and 0.5 days, respectively, to approximate the effect of mixing with soluble components. Biomass burning BC and OC are assumed to have constant solubilities of 60% and 80%, respectively.

[12] Sulfur emissions for present-day anthropogenic sources are from the Emission Database for Global Atmospheric Research (EDGAR) v3.2 1995. Black and organic carbon anthropogenic emissions for the year 1996 are from *Bond et al.* [2004]. For the sectoral experiments, emissions for BC, OC and SO_2 are partitioned into consistent sectoral categories according to their sources. Biomass burning emissions for BC and OC are based on the Global Fire Emissions Database (GFED) v1 model carbon estimates for the years 1997–2001 [e.g., *van der Werf et al.*, 2003, 2004], together with the carbonaceous aerosol emission factors from *Andreae and Merlet* [2001]. Natural and biomass burning emissions for SO_2 are described by *Koch et al.* [2006]. Natural OM emissions are assumed to be derived from terpene emissions [*Guenther et al.*, 1995], with a 10% production rate. All emissions are injected into the lowest model level except for biomass burning, which is distributed across the model boundary layer and volcanic SO_2 emissions which are as specified by the AEROCOM B model intercomparison project (http://nansen.ipsl.jussieu.fr/AEROCOM/).

3. Model Performance

[13] Our standard simulation includes all present-day emissions. To evaluate the model performance we compare with annual average sulfate, black carbon and organic matter surface concentrations in Figures 1–3. Model sulfate is evaluated extensively by *Koch et al.* [2006], however that study used the IIASA 2000 fossil fuel SO_2 emissions. Here the SO_2 fossil fuel emissions are from EDGAR 1995, which are larger, especially over Europe and east Asia. To some extent these emissions differences may result from the earlier 1995 date of the EDGAR emissions. The observations shown in Figure 1 for Europe are averages over the years 1995 to 2001, thus they fall between the dates of the 2 emission estimates. The model sulfate performance over Europe is better with the EDGAR emissions: using the IIASA emissions, the average ratio of model to observed of *Koch et al.* [2006] was about 0.6 over Europe; with the EDGAR emissions this ratio is about 0.9. However, the EDGAR emissions result in a larger positive bias for SO_2. In North America, the model sulfate tends to be deficient in the east but excessive over the west. *Koch et al.* [2006] attributes the bias, which is largest in summertime, to excessive advection westward over the Rocky Mountains (which have reduced elevation because of the coarse model resolution). Model sulfate at remote sites is generally less than observed.

[14] The model BC surface concentrations agree within a factor of 2 with observations at most sites (Figure 2), although they are clearly too small in Asia, Europe, and eastern United States, and too large at some remote sites. Similarly, model organic mass agrees with observations within a factor of 2 over most U.S. sites, but is too small over Europe and Asia (Figure 3). The scatter and bias are apparently smaller than in the previous GISS aerosol simulation [*Koch*, 2001] and those of other older models (e.g., those compared by IPCC 2001 [*Houghton et al.*, 2001]). The improvement can be attributed to some combination of emissions and model development and to the choice of annual mean recent (post late 1980s) observations.

[15] Our investigations of regional and sectoral contributions to the aerosol distributions will allow us to gain insight into the causes of the model biases.

4. Regional Emission Experiments

[16] Here we explore the impacts of aerosols emitted from major source regions (shown in Figure 4), corresponding approximately as "North America," "South America," "Europe," "Africa," "south Asia" (approximately India), and "Southeast Asia" (approximately China). Note that these labels are crude: thus, for example, North America does not include much of Mexico; Africa is drawn to include the biomass burning region only, etc. We perform multiple experiments, in each one eliminating the emissions from the source region, non-biomass-burning anthropogenic emissions from North America, Europe, south Asia and Southeast Asia and biomass burning emissions from South America and Africa. The aerosol concentrations, optical thickness and radiative forcings from each source region are found from the difference between the full simulation, including all sources, and each region elimination simulation. Eliminating regions rather than running with aerosols coming from a single region minimizes nonlinearities that would result from the sulfur chemistry. Throughout this section we will refer to "NBBA" or Non-Biomass-Burning Anthropogenic aerosols. In other studies NBBA are termed "industrial," however in this study "industrial" is one sector within NBBA.

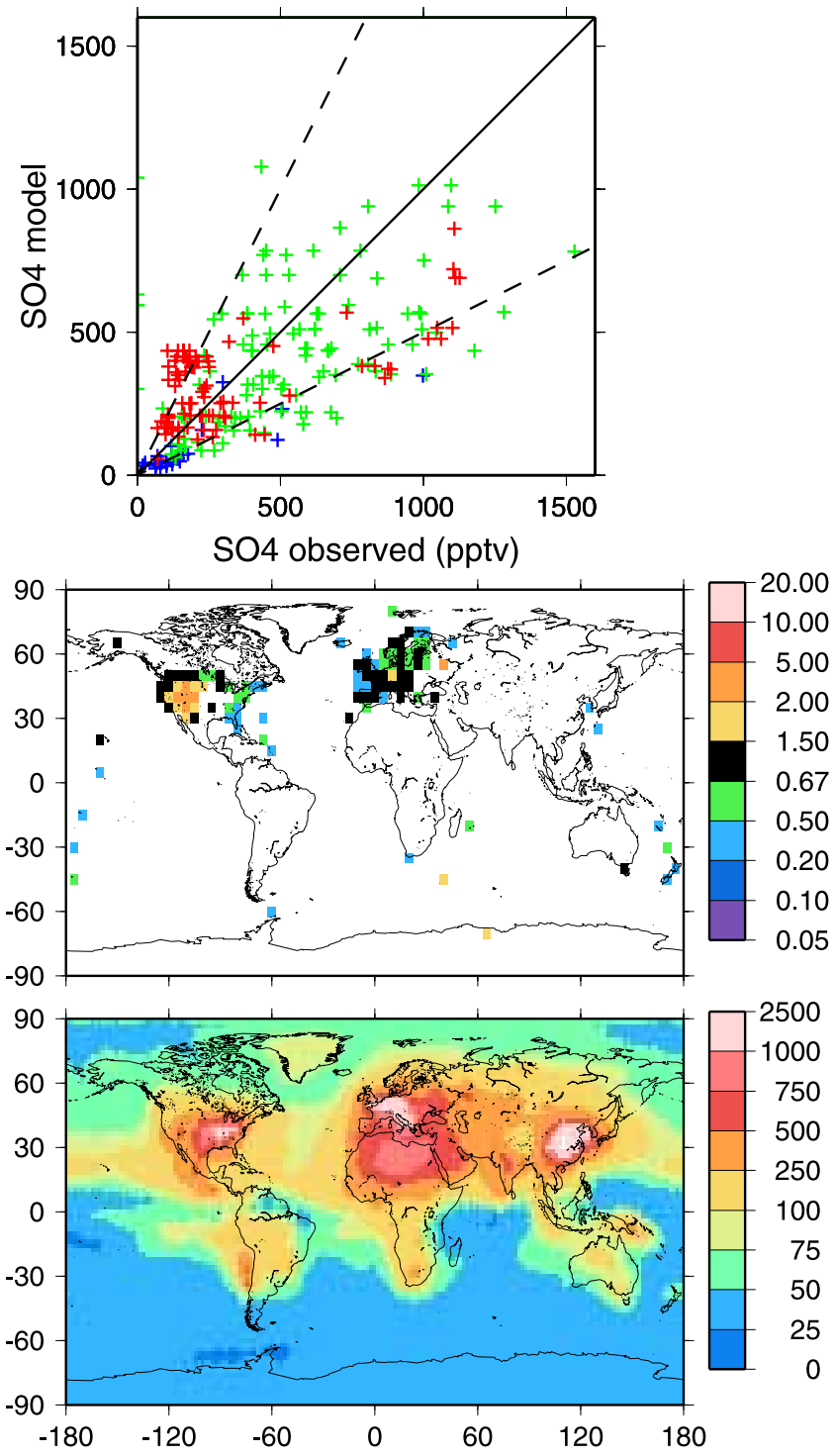

Figure 1. (top) Scatterplot of observed and modeled sulfate annual mean surface concentrations for remote sites (blue), Europe (green) and United States (red), (middle) ratio of model to observed concentrations, and (bottom) the model surface concentration. Units are pptv. Dashed line is factor of 2. European data are from EMEP, between 1995 and 2001; US data are from the IMPROVE network, between 1995 and 2003; and "Remote" data are from D. Savoie and J. Prospero (personal communication, November 1999).

[17] Table 2 shows the emissions from each region and the percent of the total emissions, for each aerosol type. Some regions are significantly more important for some aerosol types. Organic matter is derived mostly from biomass burning and from natural terpene emissions. Sulfur dioxide is derived largely from natural sources and from NBBA sources in Southeast Asia, Europe and North America. Southeast Asia is the largest regional source of NBBA

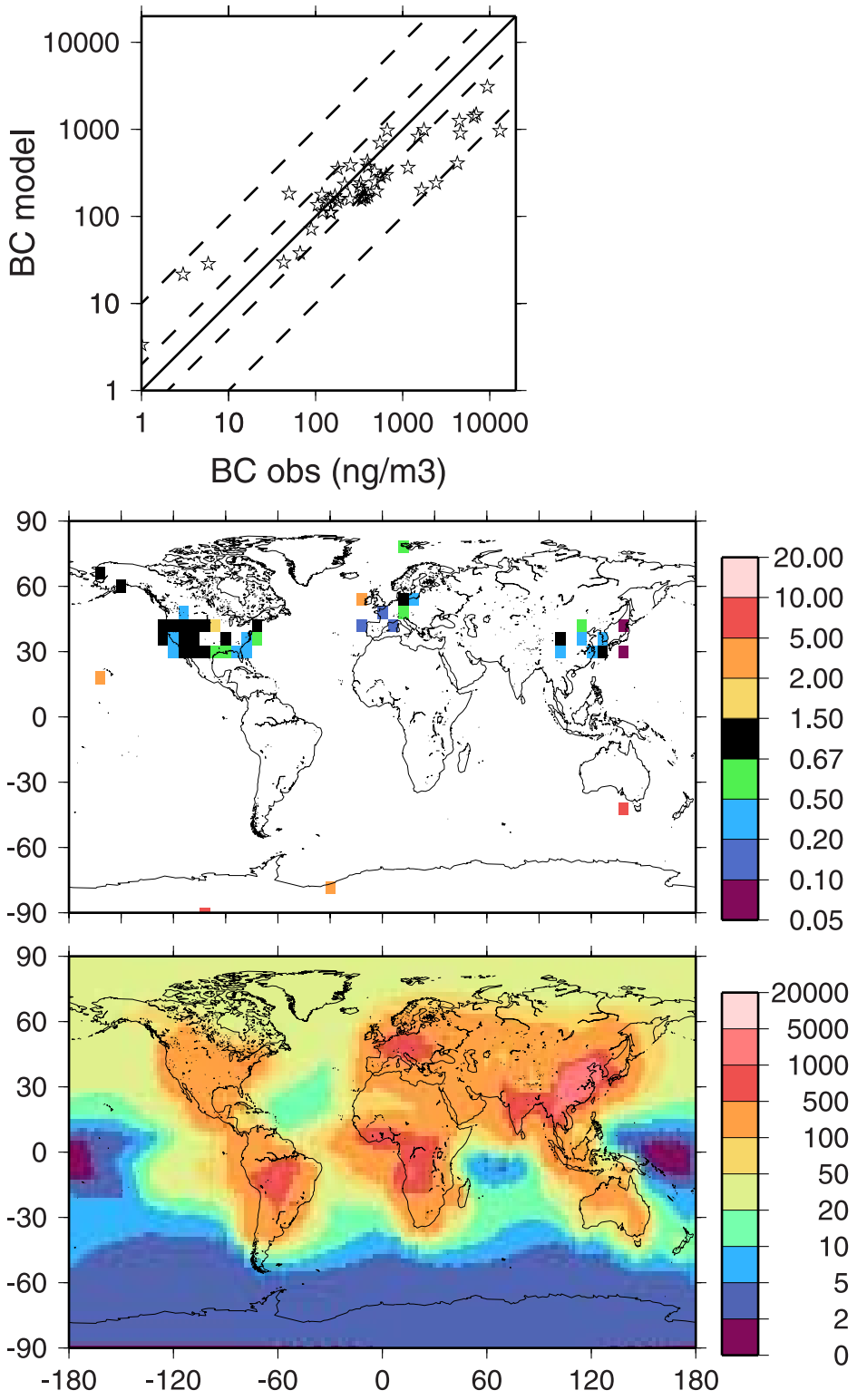

Figure 2. (top) Scatterplot of observed and modeled black carbon annual mean surface concentrations, (middle) ratio of model to observed concentrations, and (bottom) the model surface concentration. Units are ng m^{-3}. Dashed lines show factors of 2 and 10. Data include annual mean observations postdating the late 1980s and are referenced by *Koch and Hansen* [2005] plus Asian observations referenced by *Novakov et al.* [2005] and observations at Walignan, Shangdianzi, and Wenjiang (W. Wang, personal communication, October 2005).

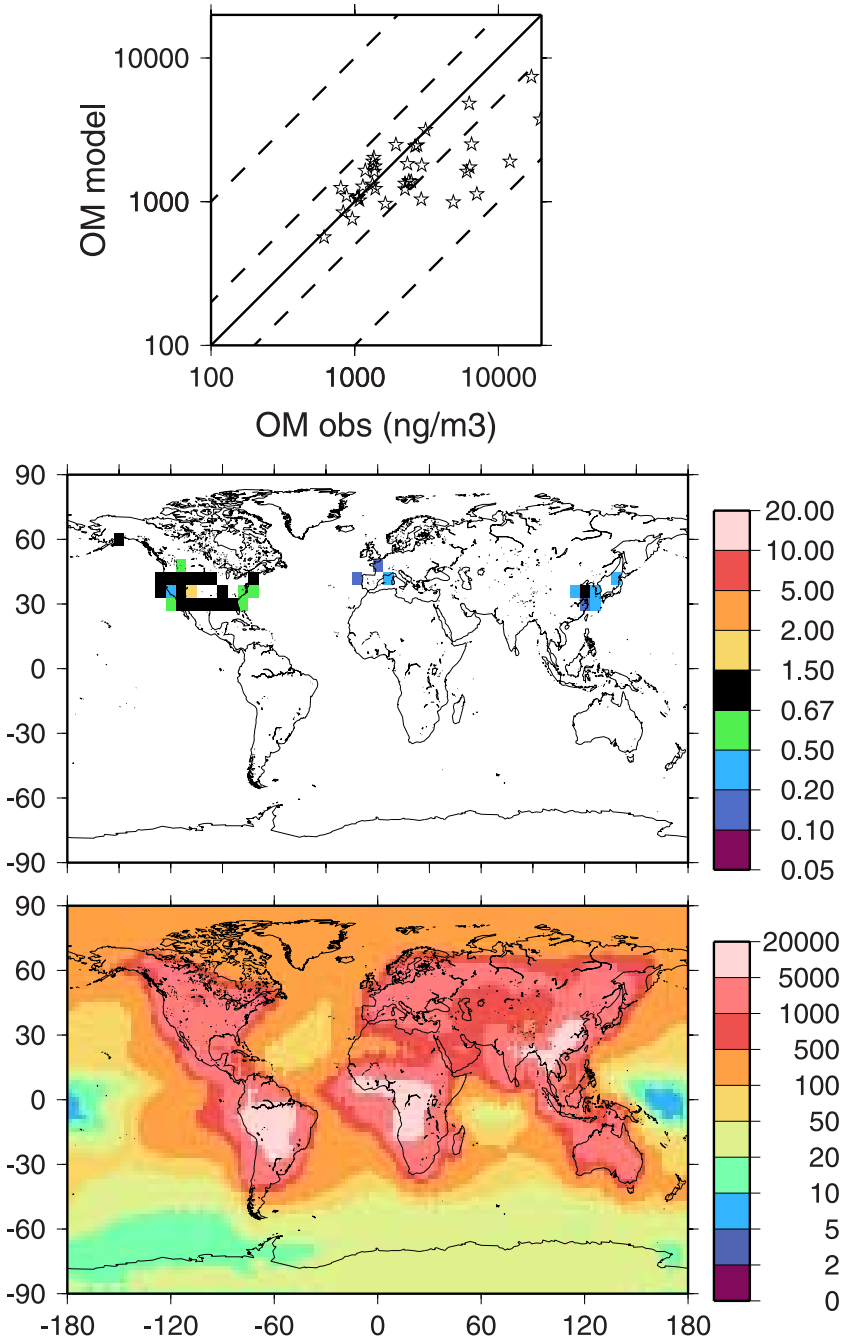

Figure 3. (top) Scatterplot of observed and modeled organic matter annual mean surface concentrations, (middle) ratio of model to observed concentrations, and (bottom) the model surface concentration. Units are ng m^{-3}. Dashed lines show a factor of 2 and 10. Data include annual mean observations postdating the late 1980s and are referenced by *Koch and Hansen* [2005] plus Asian observations referenced by *Novakov et al.* [2005].

BC. These BC emissions approximately equal those from North America, Europe and south Asia combined, or to the rest of the world's NBBA BC emissions combined, or to African biomass burning BC emissions.

[18] In Figure 5 we compare the emissions from these regions with their global (left) and local (right) loads. The left side compares the percent emitted from each region (as also given in Table 2) with the percent contribution of each region to the global burden, calculated from the regional source experiments. Note that these include only NBBA aerosols (for south Asia, Southeast Asia, North America, and Europe) or only biomass burning aerosols (for South America and Africa). In some cases, the contribution to the global burden is larger than we would infer from the emissions, such as NBBA aerosols from south Asia and biomass burning aerosols from South America. Biomass burning emissions from Africa are larger than those from South America, however the burden from South American

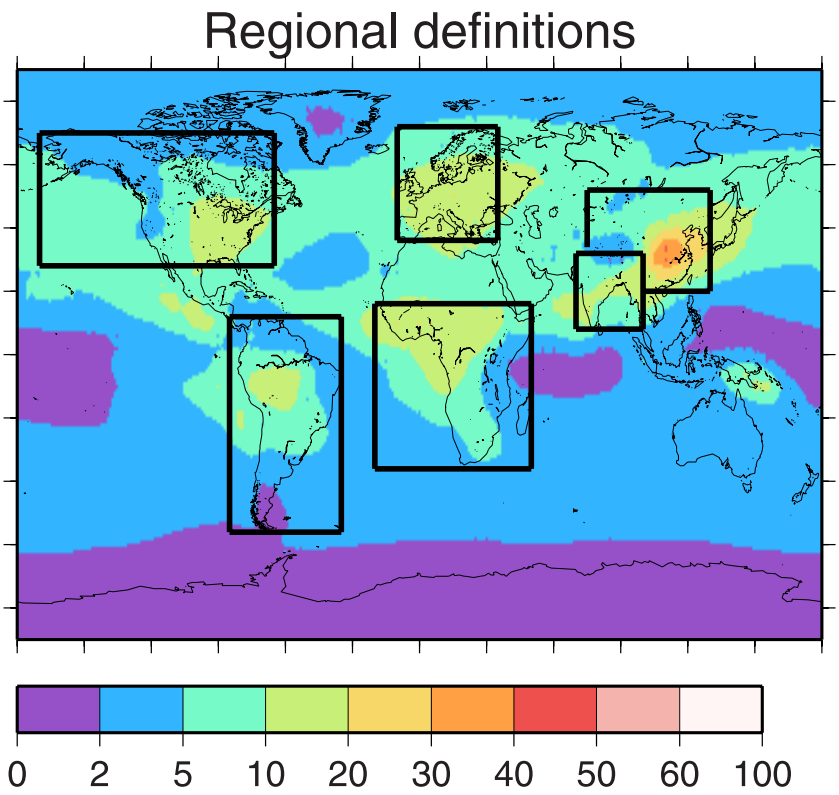

Figure 4. Regional definitions for source experiments: from left to right, North America, South America, Africa, Europe, south Asia, and Southeast Asia. Also shown is total (sulfate and carbonaceous) aerosol optical thickness × 100.

biomass burning is larger. The African biomass burning emissions are weighted more toward the equator and are more efficiently scavenged than those from South America; we will discuss this further below. In Figure 5 (right) we compare percent emitted from each region, now including all aerosols (the sum of NBBA, biomass burning and natural), and the percentage of the global burden located above each region. These are found from the full-emission experiments. Here we see that most regions emit a much larger portion than is found above their borders.

[19] We calculate percent aerosol burden exported (B_E) from the largest source regions (Table 3):

$$B_E = \frac{(B - B_R)}{B} \times 100 \quad (1)$$

where B is the burden (mass) generated by a source region and B_R is the mass that overlies the region. These burdens are taken from the regional source experiments. In most cases the larger portion of aerosol generated by a region is transported elsewhere. Southeast Asia exports about 67% and 82% of its NBBA BC and sulfate to other regions. Europe exports 67% and 89% of its NBBA BC and sulfate. India exports 80% of its NBBA BC. North America exports 68% of its NBBA sulfate. South America exports about 1/2 of its biomass burning aerosols, while Africa exports much less (11% and 17% OC and BC respectively). Note that these export amounts depend somewhat upon the size of our defined region, so that a small region box will tend to export a larger portion of its emissions while a larger region box is able to contain more of its emissions.

[20] Sulfur emissions from Southeast Asia and Europe greatly exceed the contributions to sulfate (global and regional) burden. This is because sulfate production in these regions is oxidant limited; that is, the local oxidants are not sufficient to convert the emitted SO_2 to sulfate prior to (primarily dry) deposition. Thus although SO_2 emission

Table 2. Aerosol Emissions: Regional Contributions[a]

	BC	OM	SO_2
	NBBA		
Southeast Asia	1.5 (18.3)	2.9 (4.9)	19.8 (19.1)
North America	0.4 (4.9)	0.8 (1.4)	9.6 (9.2)
Europe	0.5 (6.1)	0.9 (1.5)	16.3 (15.7)
South Asia	0.6 (7.3)	2.2 (3.8)	3.8 (3.7)
Other	1.5 (18.3)	4.7 (8.0)	22.6 (21.8)
	Biomass		
South America	1.2 (14.6)	9.6 (16.4)	0.3 (0.3)
Africa	1.5 (18.3)	11.3 (19.3)	0.6 (0.6)
Other	1 (12.2)	9.7 (16.5)	0.4 (0.4)
	Natural		
Natural	0 (0)	16.6 (28.3)	30.4 (29.3)
	Total		
Total	8.2 (100)	58.7 (100)	103.8 (100)

[a]Absolute amount in Tg (S, BC or OM) yr^{-1} with percentage in parentheses.

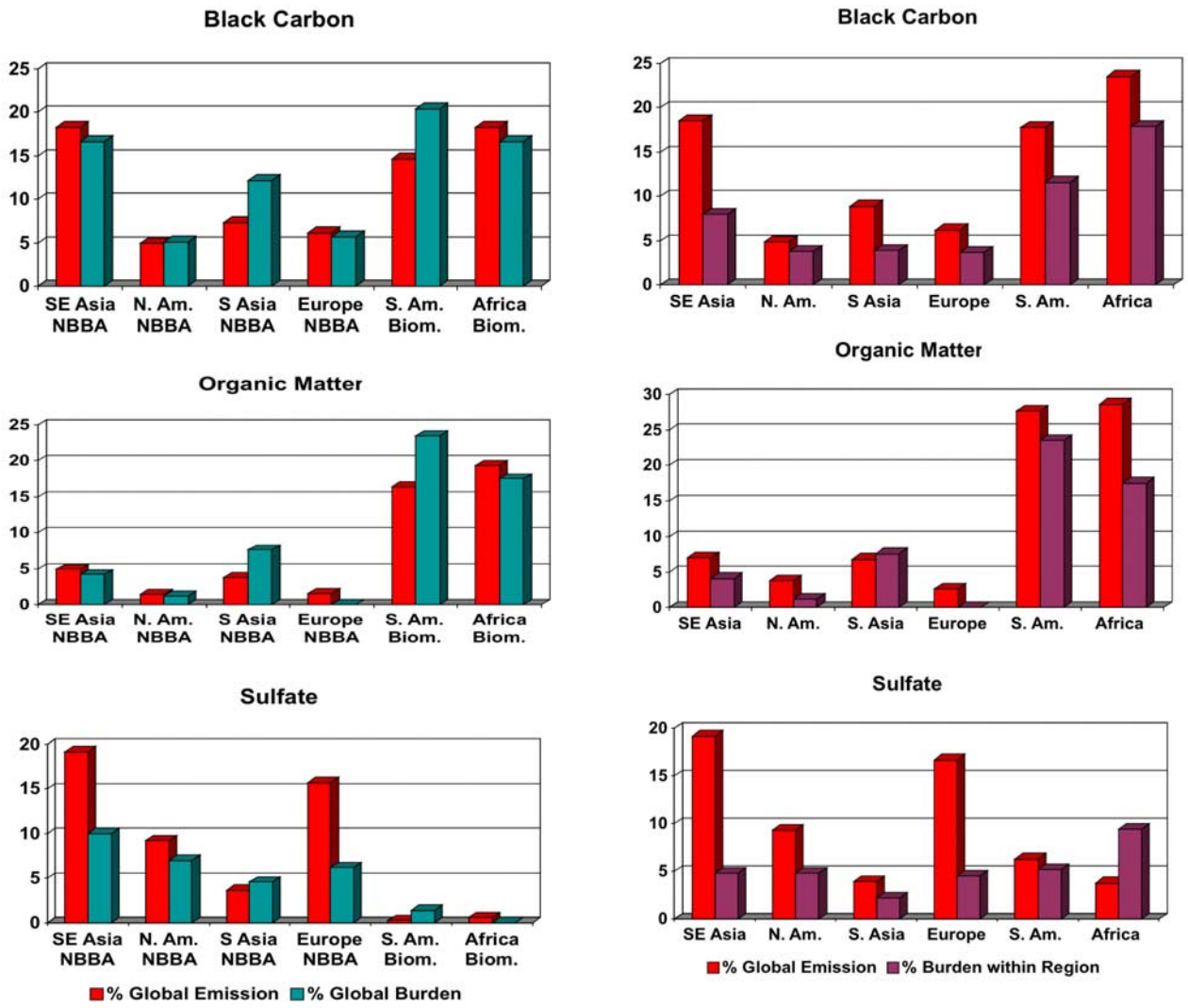

Figure 5. (left) Percent of global emission from selected regions and percent contribution of these NBBA or biomass burning emissions to global burden. (right) Percent of global emission, including all sources, from each region compared to the percent burden which overlies the region. Note that sulfate emissions are SO_2 plus sulfate, while the burdens are for sulfate.

from China and Europe is 19 and 16% of the global emission, these regions only generate 10 and 6% of the respective global burdens. Oxidant limitation probably also explains why these regions export a larger percentage of sulfate than BC (Table 3), since SO_2 from the regions tends to be exported to other regions before encountering sufficient oxidants to form sulfate.

[21] In all cases in Figure 5 (right) the percent emitted is greater than the percent burden within the region, except for sulfate in Africa and OM in India. More than half of the sulfate over Africa is imported from other regions.

[22] Figure 6 shows the zonal annual mean concentration distribution for BC and the percent contributions from the source regions. The zonal mean concentrations for OM and sulfate (not shown) are distributed similarly to BC, although biomass burning contributions to OM and sulfate are larger and smaller than BC, respectively. The regions that contribute disproportionately large amounts to the global burden are those with greatest vertical transport, such as Asia and South America. African biomass burning emissions are also lofted by convection, however they tend to remain at lower latitudes and are more efficiently scavenged by precipitation. The global mean OM biomass burning lifetimes for the full model, the model without African biomass burning and the model without South American biomass burning are 6.2 days, 6.6 days and 5.2 days, respectively. Thus we see that the African biomass burning OM has

Table 3. Percent Aerosol Burden Exported[a]

	BC	OM	Sulfate
Southeast Asia NBBA	67	NA	82
North America NBBA	NA	NA	68
Europe NBBA	67	NA	89
South Asia NBBA	80	NA	NA
South America biomass	53	50	NA
Africa biomass	17	11	NA

[a]Calculation for regions with >5% global emission.

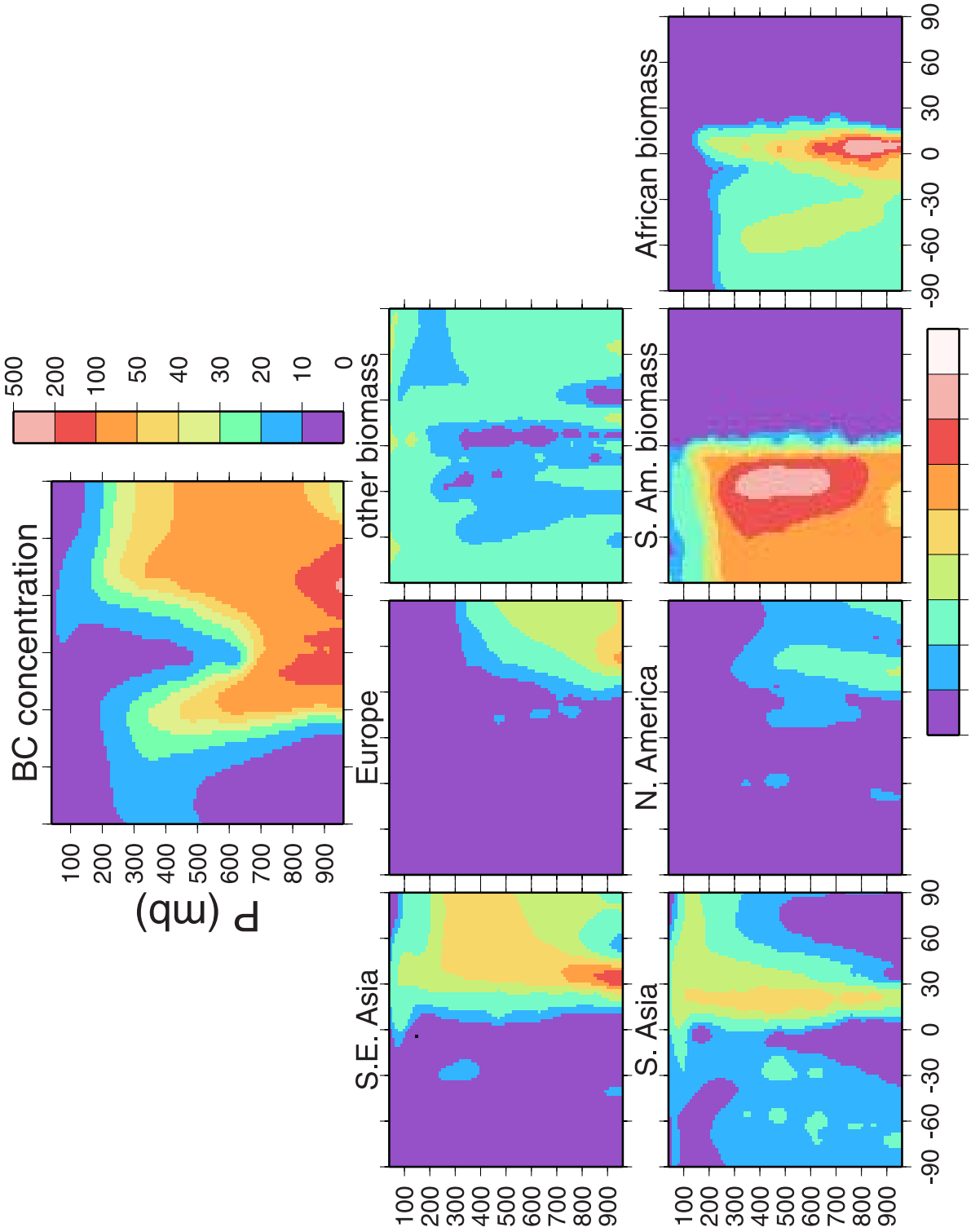

Figure 6. (top) Annual zonal mean BC concentration (ng m^{-3}). (bottom) Percent contributions from regions. The left four plots are NBBA emissions only, and the right three plots are biomass burning emissions only.

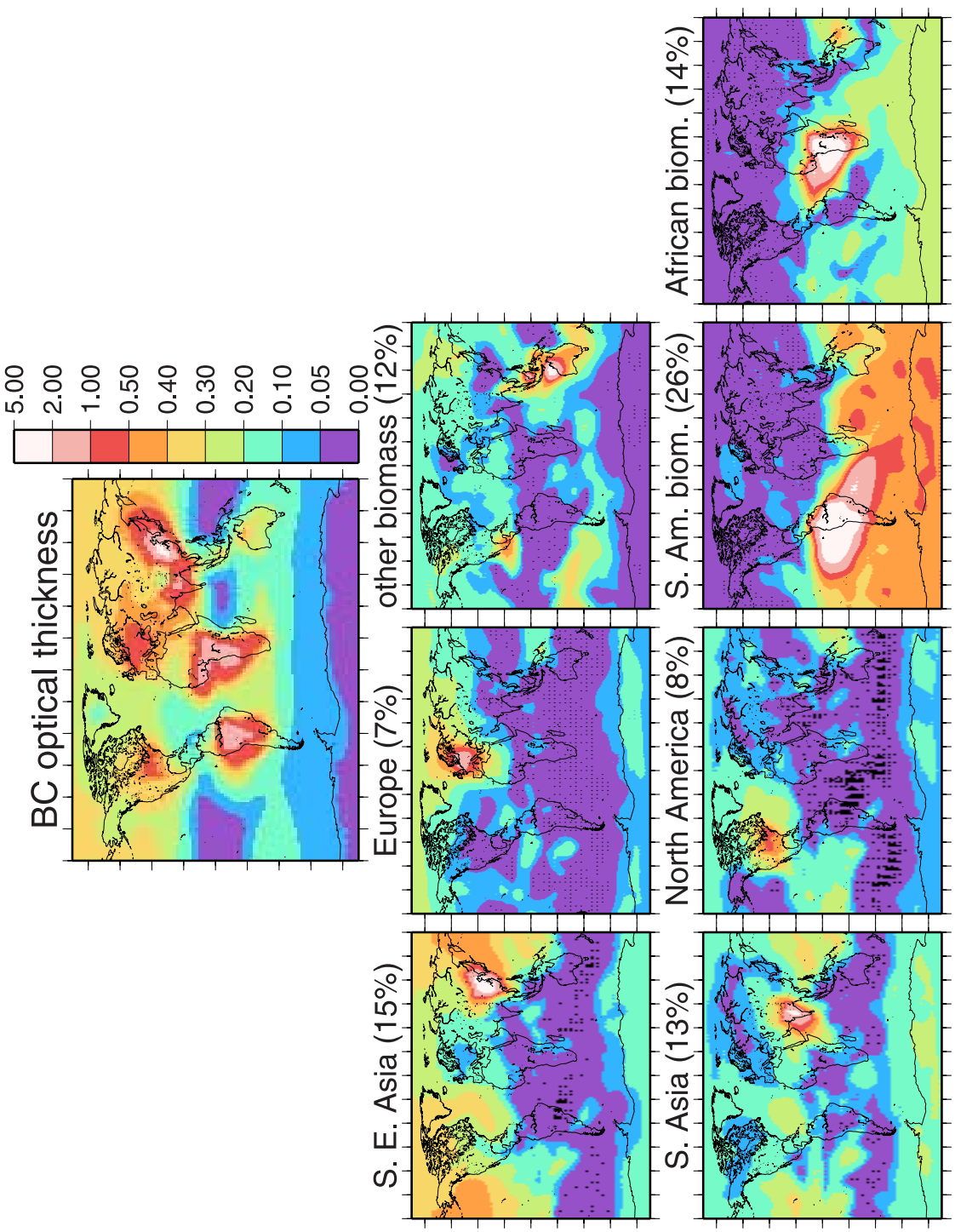

Figure 7. (top) Annual mean BC optical thickness (×100). (bottom) Percent contributions from regions. The left four plots are NBBA emissions only, and the right three plots are biomass burning emissions only. Global mean percent contributions are given in parentheses.

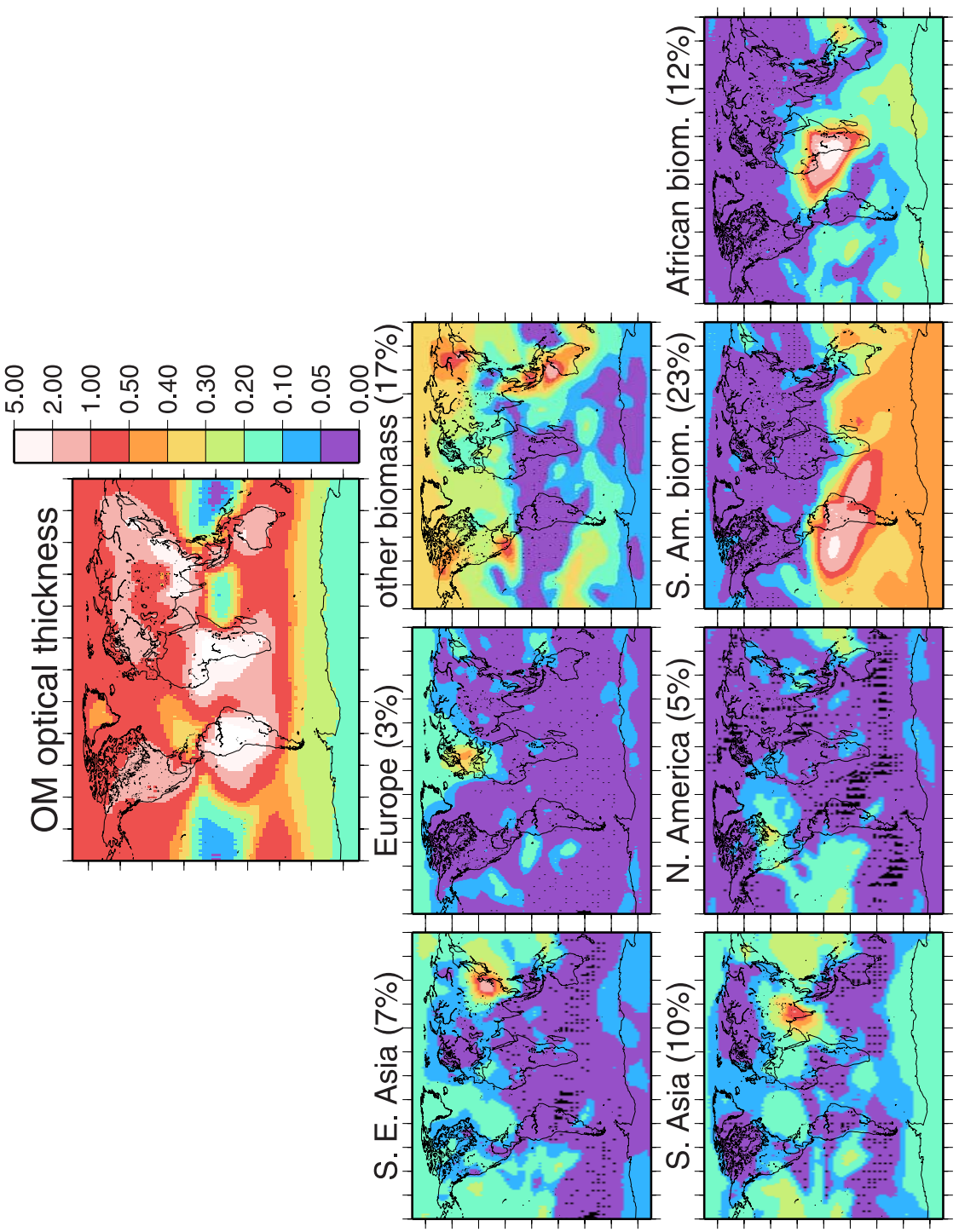

Figure 8. (top) Annual mean OM optical thickness ($\times 100$). (bottom) Percent contributions from regions. The left four plots are NBBA emissions only, and the right three plots are biomass burning emissions only.

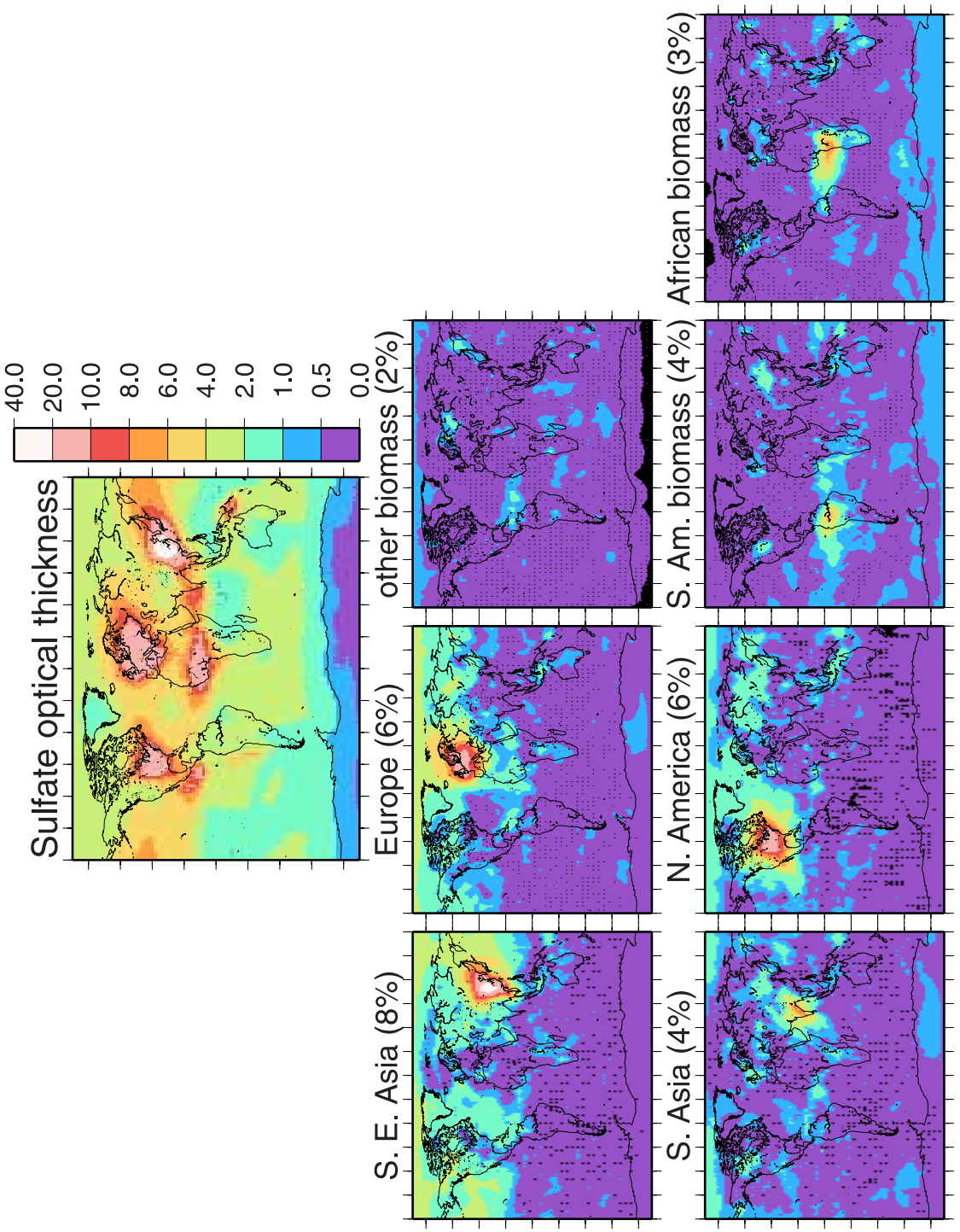

Figure 9. (top) Annual mean sulfate optical thickness ($\times 100$). (below) Percent contributions from regions. The left four plots are NBBA emissions only, and the right three plots are biomass burning emissions only.

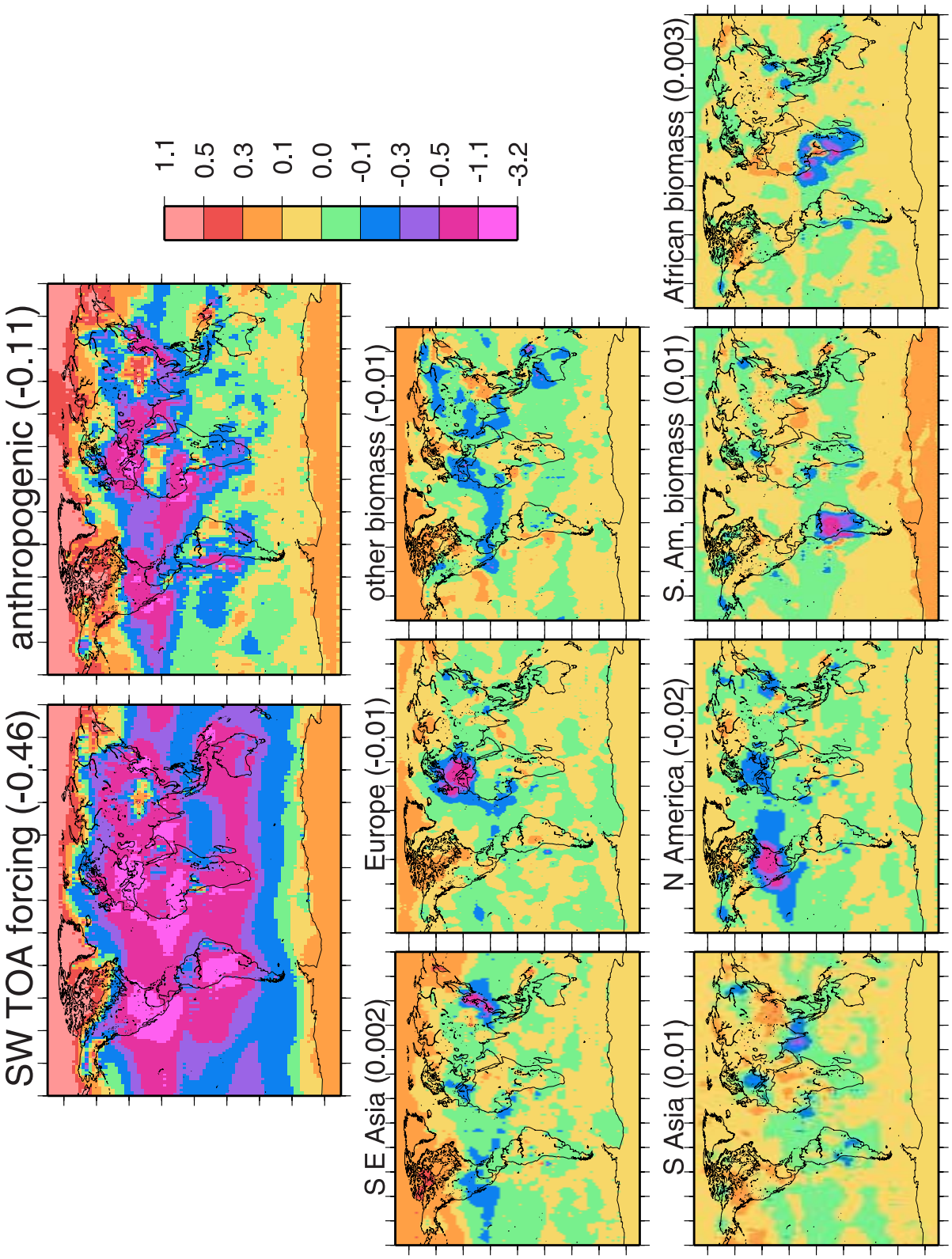

Figure 10. (top) Annual mean short-wave TOA forcing from (left) natural plus anthropogenic and (right) anthropogenic. (bottom) Contributions from regions. The left four plots are NBBA emissions only, and the right three plots are biomass burning emissions only.

Table 4. Aerosol Forcings: Regional Contributions[a]

	BC	OM	Sulfate
	NBBA		
Southeast Asia	6.3 (20)	−0.41 (2)	−5.6 (9)
North America	1.9 (6)	−0.21 (1)	−4.2 (7)
Europe	2.2 (7)	0.25 (−1)	−3.4 (6)
South Asia	4.8 (15)	−1.3 (7)	−2.3 (4)
	Biomass		
South America	6.4 (20)	−4.7 (25)	−0.84 (1)
Africa	4.4 (14)	−3.7 (19)	−0.40 (1)

[a]×100 W m^{-2}. Percentage in parentheses is relative to total TOA forcing for each species.

shorter lifetime than the global mean biomass OM, while South American biomass burning has longer lifetime.

[23] Figures 7–9 are the optical thickness distributions and the percent derived from each region for BC, OM and sulfate. Figures 7–9 show the pollution export from the regions. *Koch and Hansen* [2005] showed that the largest portion of BC in the Arctic was derived from south Asia, which included most of China and India. In the current study Southeast Asia and south Asia regions are distinguished and we see that the region which includes much of China contributes the largest portion of Arctic BC. The BC from India, while dispersed widely, remains mostly at lower latitudes. As discussed by *Koch and Hansen* [2005], the BC from Southeast Asia travels to the Arctic in the mid and upper troposphere. Closer to the surface European NBBA sources are dominant. Similarly, Arctic sulfate comes mostly from Southeast Asia and Europe, with the latter dominating close to the surface. In contrast, Arctic OM comes mostly from "other" biomass burning, primarily from the Pacific northwest and from Siberia.

[24] In the Southern Hemisphere, the model indicates that South American biomass burning aerosols dominate the carbonaceous load in Antarctica and throughout most of the remote Southern Hemisphere. The model may exaggerate this dominance because model precipitation is less than observed in south-central South America [*Schmidt et al.*, 2006; *Koch et al.*, 2006]. However, the largest precipitation bias, about 50% less than observed, is during summertime. During springtime, when South American biomass burning is largest, the bias is primarily to the south of the major burning regions [*Koch et al.*, 2006]. We also note that estimation of biomass burning emissions in South America is particularly problematic [*Giglio et al.*, 2006].

[25] As shown above (Figure 5), the sulfate over Africa is derived from nonlocal sources. In Figure 9 we see that some (5–20%) of the African sulfate comes from Europe. We find other instances of long-range transport among regions. For example, 20–30% of BC in western North America comes from Southeast Asia. Most of the BC over Russia is from Europe and Southeast Asia. North America has more OM from biomass burning than from local NBBA sources, although our simulations do not allow us to determine the origin of the biomass burning.

[26] Figure 10 shows the annual mean, top-of-the-atmosphere (TOA), instantaneous short-wave radiative forcing. The top left plot is the forcing for all (carbonaceous and sulfate) aerosols, including natural. The annual global mean forcing is −0.47 W m^{-2}: −0.60 W m^{-2} from sulfate, −0.19 W m^{-2} from OM and 0.32 W m^{-2} from BC. The top right plot shows the anthropogenic forcing, found from taking the difference with a natural aerosol simulation, assuming that 25% of the biomass burning aerosols are natural. The annual global mean anthropogenic forcing is −0.11 W m^{-2}, −0.29 W m^{-2} from sulfate, −0.06 W m^{-2} from OM and 0.24 W m^{-2} from BC. Figure 10 (bottom) shows the contributions (to the total forcing) from the regional experiments. Table 4 provides the forcing amounts due to each component from each region. The total forcing from our regions is small compared to the total anthropogenic forcing. The total BC forcing (0.152 W m^{-2}) and sulfate forcing (−0.155 W m^{-2}) from these regions approximately cancel one another. Our regions contain 69% of the NBBA SO_2 emission, but since these are large industrial source regions, oxidant limitation results in generation of only 57% of the global NBBA burden (see also the comparison of regional emissions and burden from regions in Figure 5 (right)). On the other hand, our regions have 66% of the non-biomass BC but 72% of this BC burden, presumably because of variations in regional removal. Forcing disparities are even slightly greater, so that we have only 54% of the global NBBA sulfate forcing but 75% of the global NBBA BC forcing.

[27] Typically the aerosols are scattering near the source regions. The longer-lived absorbing aerosols can travel poleward where their radiative impact is enhanced (above the high-albedo snow/ice surfaces). Note that the organic aerosol forcing out of Europe is positive, this is because of poleward transport over icy surfaces where OM absorption is enhanced (see also Figure 8).

[28] By comparing the percent of radiative forcing due to regional emissions (shown in parentheses in Table 4) with percent emitted from each region (in parentheses in Table 2) we can learn the degree of linearity between emissions and forcing. The radiative forcing disparity with emissions generally corresponds to the optical thickness disparity. Thus the forcing of carbonaceous aerosols from south Asia is about double what we expect from the emissions. The sulfate forcing from Europe and Southeast Asia are about 1/3 and 1/2 what we expect from SO_2 emitted. South American biomass burning carbonaceous aerosol forcings exceed what would be inferred from emissions, by 30% and 55% for BC and OM respectively. African biomass burning BC forcing is somewhat (20%) less than expected from emissions. These results indicate that a single global proportionality between emissions and forcing cannot be applied to individual regions. Local differences in transport, chemistry and removal generate differences among lifetimes

Table 5. Aerosol Emissions: Sectoral Contributions[a]

	BC	OM	SO_2
Industry	1.1 (13)	1 (2)	34 (33)
Residential	2.1 (26)	8 (14)	7 (7)
Power	0.03 (0.4)	0.03 (0)	26 (25)
Transport	1.3 (16)	1 (2)	6 (6)
Biomass	3.7 (45)	30.1 (52)	2 (2)
Natural	0.0 (0)	18.6 (31)	29 (28)
Total	8.2	58.7	104

[a]Absolute amount in Tg (S, BC or OM) yr^{-1} with percentage in parentheses.

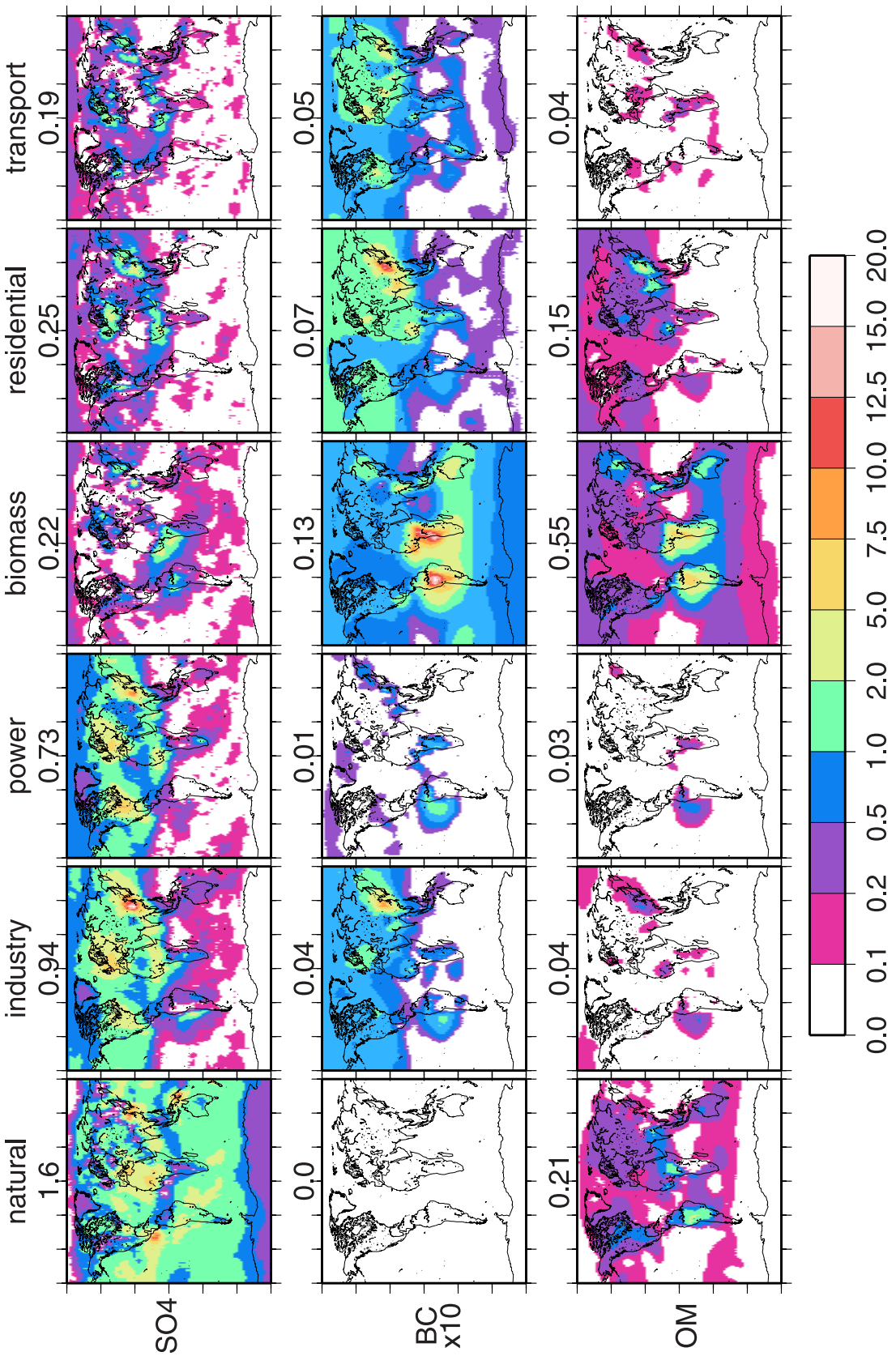

Figure 11. Annual mean optical thickness contributions from each sector for each species ($\times 100$). For BC, τ is increased by a factor of 10. Global mean value appears above each panel.

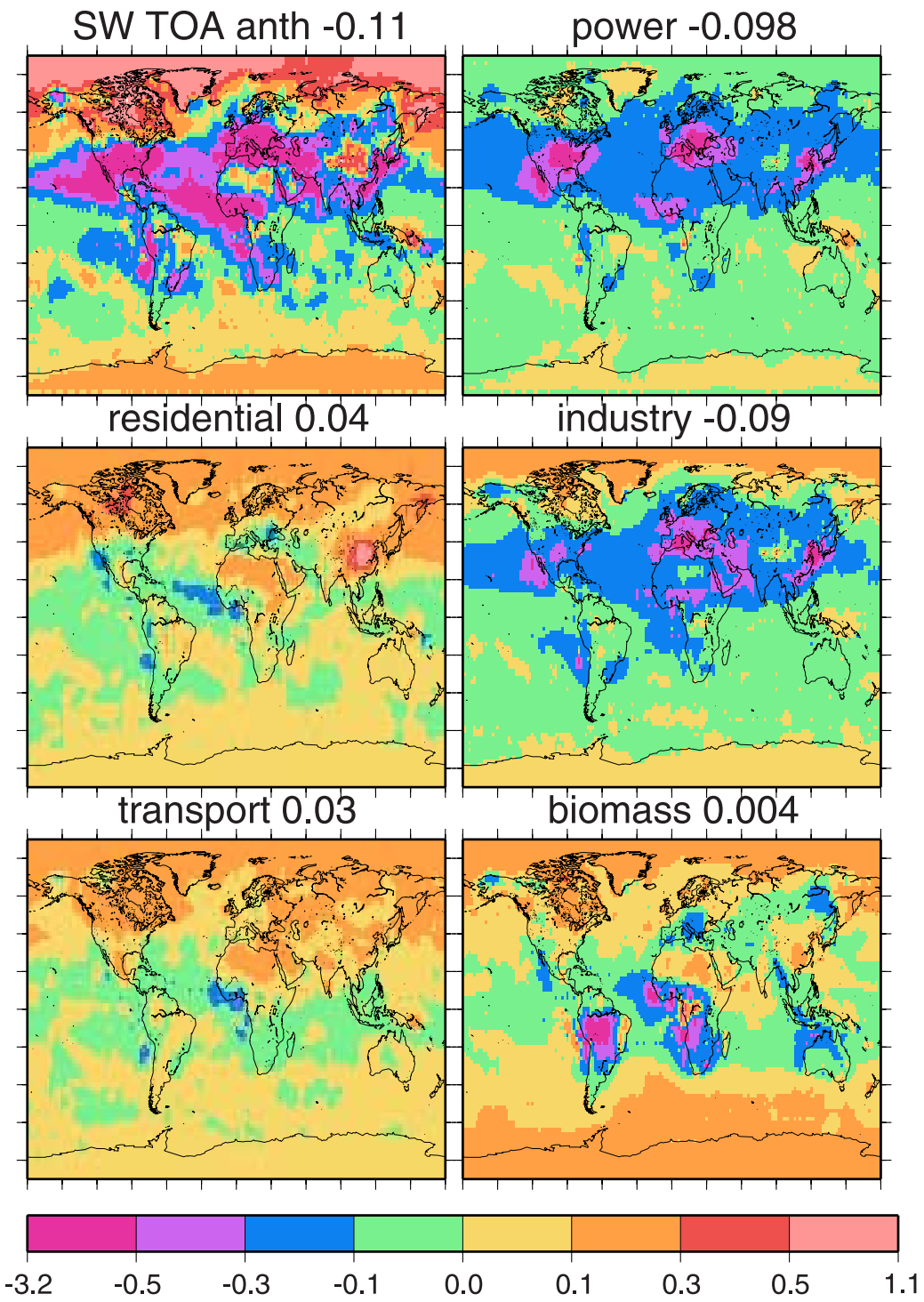

Figure 12. Annual mean anthropogenic radiative forcing from all (sulfate and carbonaceous) aerosols (top left plot) and the contributions from each sector. Global mean contribution is given. Units are W m^{-2}.

and radiative forcings of aerosols emitted by particular regions.

5. Sectoral Experiments

[29] Now we consider the influence of individual source types on aerosol distribution, load and radiative impacts. Table 5 shows the division of emissions into major sectors. Most sulfate comes from natural sources and the industrial and power sectors. Organic matter comes primarily from biomass burning, natural sources and the residential sector. Black carbon comes mostly from biomass burning, residential and transport sectors. Similar to the regional experiments, we run the model repeatedly, each time eliminating one sector. The concentrations, optical thickness and radiative forcing for each sector comes from the difference between the full run and the run with the sector eliminated.

Table 6. Aerosol Forcings: Sectoral Contributions[a]

	BC	OM	Sulfate
Industry	4.6 (13)	−0.26 (1)	−13.0 (22)
Residential	9.4 (28)	−2.2 (12)	−3.2 (5)
Power	0.4 (1)	0.0 (0)	−10.2 (17)
Transport	5.6 (16)	−0.43 (2)	−2.0 (3)
Biomass	14.3 (42)	−11.0 (58)	−2.9 (5)
Natural[b]	0.0 (0)	−5.1 (27)	−29 (48)

[a] $\times 100$ W m^{-2}. Percentage in parentheses is relative to total TOA forcing for each species.
[b] Natural does not include biomass burning.

[30] Figure 11 shows the resulting optical thickness distributions for each sector and species. Power and industry sulfate are derived from all large industrial regions of the Northern Hemisphere, and are spread across the hemisphere. Residential carbonaceous aerosols, derived mostly from Asian sources, spread over the North Pacific and into the Arctic. Transport BC is somewhat more confined to the ontinental source regions. Biomass burning carbonaceous aerosols form a band around the central Southern Hemisphere.

[31] Using these distributions and the model-observation disparities shown in Figures 1–3, we speculate about possible errors in emissions originating from particular sectors. As shown in Figures 2 and 3, the carbonaceous aerosols are underestimated by the model in east Asia (model/observed is 0.4 for both OM and BC) and in Europe (ratio is 0.9 for BC, 0.2 for OM). The carbonaceous aerosol model agrees better in North America, including Alaska. The model BC is too large for most of the few Southern Hemisphere locations, where we have no OM data. Since the residential sector is an important source of aerosol emissions in Asia and it is considered to be especially uncertain [*Bond et al.*, 2004], we suggest that increasing residential emissions would improve the carbonaceous aerosol model bias in Asia without degrading the model performance elsewhere. The overprediction of BC at high latitudes in the Southern Hemisphere may result from excessive biomass burning aerosols from South America due to deficient precipitation there (as discussed in the previous section). The model sulfate deficiencies in remote regions are probably related to errors in the natural sources

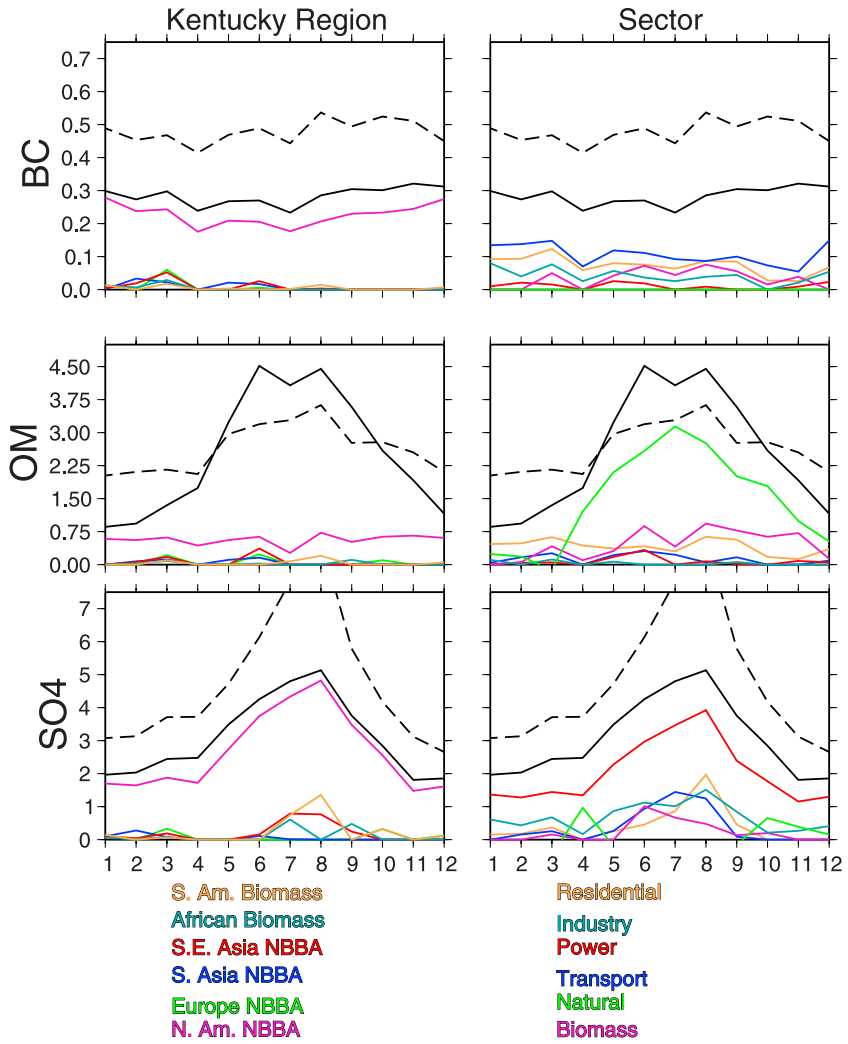

Figure 13. Comparison of model (solid black) and observed (dashed) seasonal concentrations of BC, OM, and sulfate (μg m^{-3}) in Mammoth Cave, Kentucky. The colored lines show model estimated contributions from various (left) regions and (right) sectors. Data are from the IMPROVE network (1995–2001).

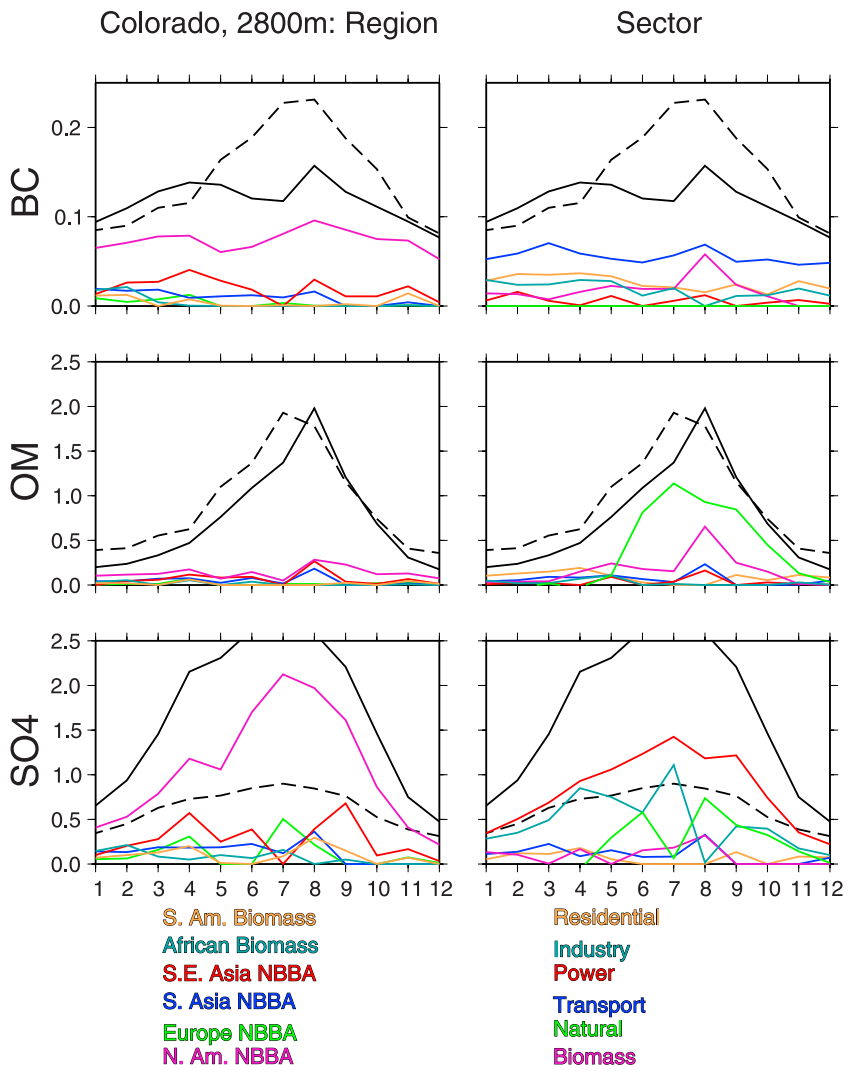

Figure 14. Comparison of model (solid black) and observed (dashed) seasonal concentrations of BC, OM, and sulfate (μg m^{-3}) at Rocky Mountain National Park, 2800 m. The colored lines show model estimated contributions from various (left) regions and (right) sectors. Data are from the IMPROVE network (1995–2001).

[*Koch et al.*, 2006]. Larger natural sulfur sources would also increase sulfate concentrations on the east coast of the U.S. where the concentrations are too small.

[32] Because BC absorbs radiation and contributes to net warming, it has been considered as a possible target to combat global warming [e.g., *Jacobson*, 2002; *Bond and Sun*, 2005]. To do so, we might hope to target sectors with large BC components compared with scattering. In Figure 12 we show the model's aerosol radiative forcing associated with the sectors. The forcing from each species in each sector is given in Table 6. The residential and transport sectors have net positive forcing and are thus potential targets for reducing global warming. If we were to eliminate emissions from the residential or transport sectors, the radiative forcing would be reduced by 0.04 and 0.03 W m^{-2} respectively. Yet the BC contribution to the forcings from these sectors is substantial: the residential forcing is composed of 0.09 W m^{-2} from BC and -0.05 W m^{-2} from OM and sulfate; the transport forcing consists of 0.06 W m^{-2} from BC and -0.03 W m^{-2} from OM and sulfate. Even in these sectors with relatively smaller scattering components, there is sufficient scattering to cancel about 1/2 of the positive forcing. Thus optimal decrease in the warming effects of aerosols might be achieved by targeting subsectors, such as diesel and perhaps coal, which have relatively large BC emissions and absorption relative to scattering.

[33] Net negative forcing results from the power and industry sectors, which have large SO_2 emissions. From Figure 12 we see that the negative forcing over low-mid latitudes of the Northern Hemisphere comes primarily from the power and industry sector aerosols. The power sector has essentially zero absorbing component. The industry sector consists of 0.05 W m^{-2} from BC and -0.14 W m^{-2} from the scattering components. These sectors cause significant negative forcing over central latitudes of the Northern Hemisphere.

[34] In Figure 12 we also see that particularly strong absorption from residential emissions occurs over Southeast Asia. Figure 11 shows that the largest positive forcing in the Arctic comes from residential BC, which the previous

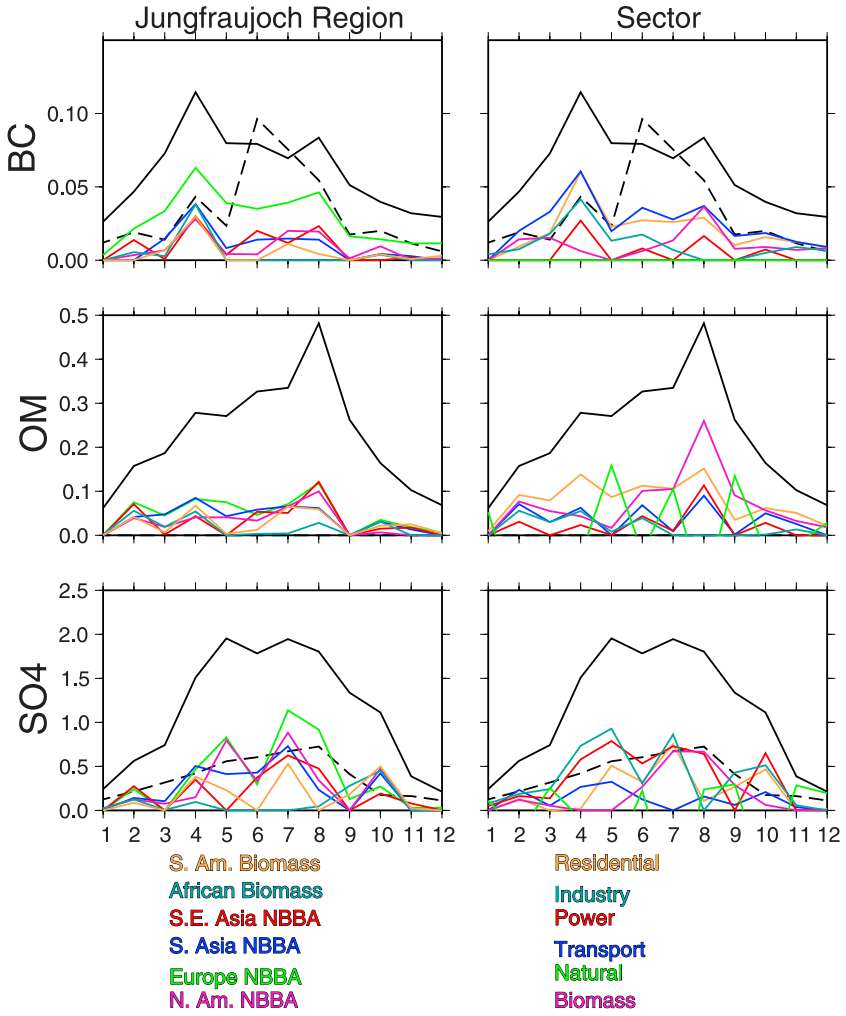

Figure 15. Comparison of model (solid black) and observed (dashed) seasonal concentrations of BC, OM, and sulfate (μg m^{-3}) at Jungfraujoch, 3450 m. The colored lines show model estimated contributions from various (left) regions and (right) sectors. Data are from 1995 to 1996 (EMEP [*Nyeki et al.*, 1998]).

section suggests were probably derived from Southeast Asia. If indeed Southeast Asian residential emissions are underestimated, the positive forcing in the Arctic may also be underestimated.

[35] Comparison of the percent emitted in each sector (Table 5) with the load percentage (Figure 11) or the forcing (Table 6) indicates the degree of linearity between sectoral emissions and impacts. As we learned in the previous section, sulfate load is often not linearly related to SO_2 emissions, due mostly to oxidant limitation in regions such as Southeast Asia and Europe. Indeed here we see that the industry and power sectors contribute 24% and 19% to the sulfate optical thickness, less than we expect from the 33% and 25% contributions to SO_2 emissions. The natural and biomass burning sulfate have larger burden (40% and 6%) than expected from emissions (28% and 2%). These components have longer lifetime because of the higher altitude of precursor emission [*Koch et al.*, 2006]. The carbonaceous aerosol load and forcing are generally more correlated with emissions. However, the biomass burning OM load and forcing percentages (58%) are larger than would be expected from emissions (52%) and the BC is somewhat less. This comes primarily from the enhanced burden for South American biomass burning OM. Also, the ratio of the emission factors assumed for OM/BC is larger for extratropical forest fires (15) than for tropical biomass burning (8) [*Andreae and Merlet*, 2001]. Thus fires in high latitudes, such as Siberia and the Northwest Territories, have larger OM/BC. It is possible that these aerosols have longer lifetime and contribute to the larger biomass burning OM forcing relative to emission percentage.

6. Seasonality at Particular Locations

[36] We now consider the seasonalities of regional and sectoral contributions at a selection of locations where we have data for at least 2 species to compare with the model. Our natural and biomass burning emissions have seasonal variability, however the NBBA emissions do not. We will see the degree to which the model captures observed seasonality. We sought data near our source regions and polar regions, and will show comparisons in eastern and western United States, Europe, Southeast Asia, near the Arctic and in Antarctica.

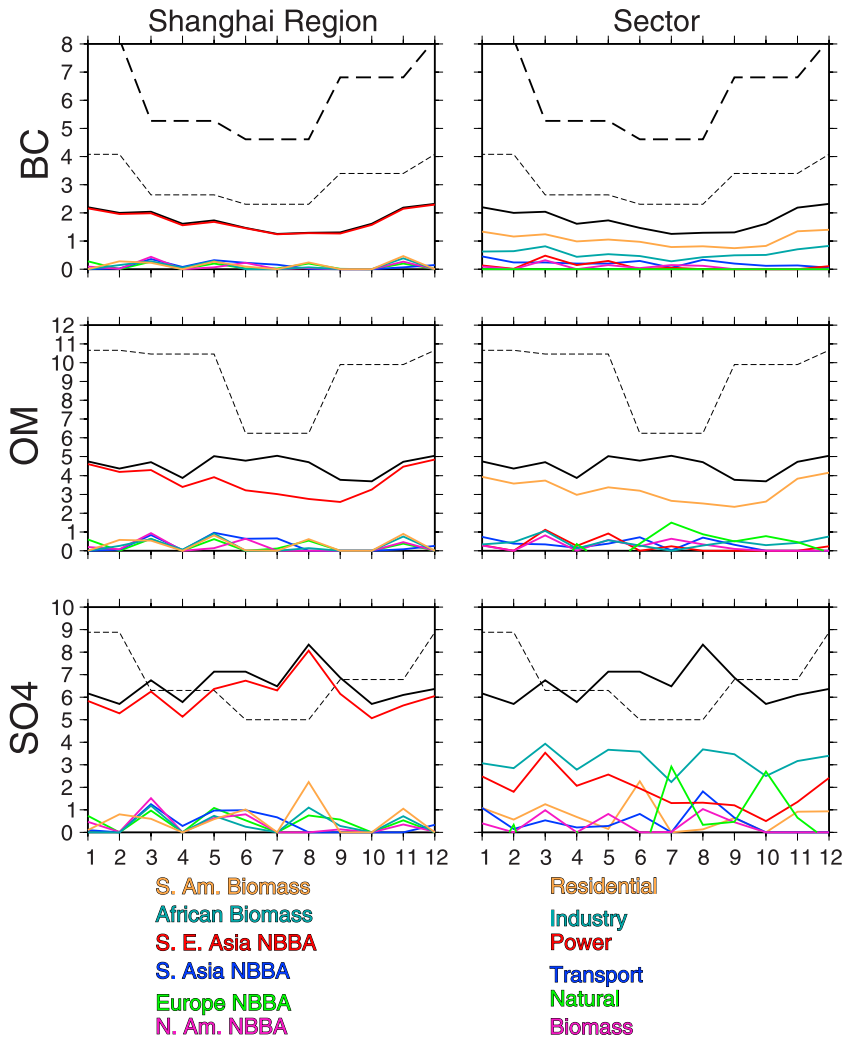

Figure 16. Comparison of model (solid black), observed (dashed), and observed/2 (light dashed) seasonal concentrations of BC, OM, and sulfate (μg m^{-3}) at Shanghai, China. The colored lines show model estimated contributions from various (left) regions and (right) sectors. Data are for winter, spring, summer, and fall of 1999–2000, from *Ye et al.* [2003].

[37] Figure 13 shows the seasonality at an eastern U.S. location, Mammoth Cave, Kentucky (IMPROVE data). As shown in section 3, in this region the model has deficient BC and sulfate. The seasonalities are reproduced in the model, except that the magnitude of the OM seasonality is greater than observed. Perhaps model terpene and/or biomass burning is overpredicted during summertime, while NBBA sources are less than they should be. Larger NBBA emissions would improve the model simulation of BC, sulfate and wintertime OM. The model indicates some sulfate transport from other regions during summertime.

[38] Figure 14 has seasonality for the high-altitude Rocky Mountain State Park IMPROVE site. The model underestimates BC in the summertime and overestimates sulfate, especially during summer. Black carbon is derived mostly from the transport sector with lesser amounts from residential, biomass burning and industrial sources, with minimal model seasonality. Local fire and diesel sources in the park would not be resolved in the model and may explain some of the summertime BC model underestimate. On the other hand, OM is successfully modeled. Here and in many of the central and western U.S. sites the model OM indicates dominance of natural and biomass burning sources and the model agreement with observations is good. Sulfate comes primarily from power generation, with contributions from industry and natural sources. Since this is a high-elevation site, the model detects transport of sulfate and BC from other regions, such as Southeast Asia, especially during spring and fall.

[39] Figure 15 shows BC and sulfate data at another high-altitude (3400 m) site, Jungfraujoch, Switzerland. The model and data show maxima in summertime, but the model overestimates BC and sulfate. According to the model, although the European sources dominate, the aerosols here are derived from many regions, especially during spring and summer. The NBBA components are dominant for sulfate and BC. NBBA emissions do not include seasonality, so the modeled seasonal variability at Jungfraujoch is due primarily to increased vertical transport during summertime.

[40] Figure 16 shows seasonality for Shanghai, China. As discussed in section 3, the model greatly underestimates the aerosol amounts in Southeast Asia. We see this here again:

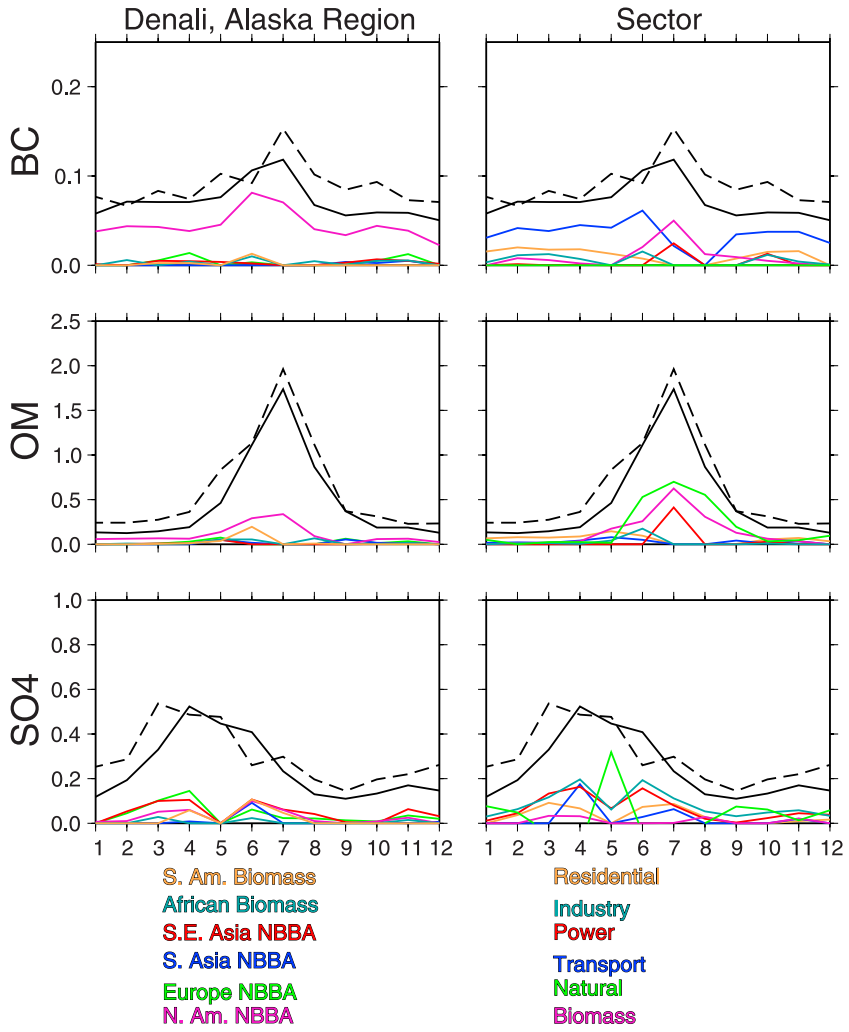

Figure 17. Comparison of model (solid black) and observed (dashed) seasonal concentrations of BC, OM, and sulfate (μg m^{-3}) at Denali, Alaska. The colored lines show model estimated contributions from various (left) regions and (right) sectors. Data are from the IMPROVE network (1995–2001).

model sulfate is too small by about a factor of 2 and carbonaceous aerosols by a factor of 3–4. At Shanghai the bias is especially large because we compare urban observations with a model grid box average. The observed seasonality indicates maximum aerosol amounts during winter. Model seasonality is reproduced for BC but not OM and sulfate. Some of the modeled sectors, such as residential carbonaceous, industrial BC, and sulfate from power, contain wintertime maxima. Such maxima would come from increased boundary layer stability during winter. However aerosol seasonality in Shanghai is thought to come from a combination of meteorology and wintertime increases from heating fuels [*Ye et al.*, 2003]. Indeed it appears that the model seasonality would improve if we included information on heating fuel variability.

[41] Finally we consider seasonality at two high-latitude remote sites, Denali Alaska (Figure 17) and Neumayer Antarctic (Figure 18). Denali has summertime peaks in carbonaceous aerosols and a springtime peak in sulfate; the model simulates these seasonalities quite well. Most of the BC is from the North American transport sector, however the summertime peak is derived from biomass burning. Similar to the Rocky Mountain site, OM seasonality comes mostly from natural and biomass burning sources. Sulfate comes primarily from the industry and power sectors, with some significant springtime sources as far away as Europe and Southeast Asia.

[42] In Neumayer (Figure 18) the carbonaceous aerosols peak in springtime, when biomass burning aerosols are maximum. The model overestimates the BC peak. As already discussed, South American biomass burning is the largest source of Antarctic aerosols, followed by African biomass burning. During springtime when the polar vortex weakens carbonaceous aerosols from as far away as south Asia descend over the continent. Some springtime aerosols are derived from the transport and residential sectors. Sulfate peaks during summertime and is dominated by the natural DMS source.

7. Conclusions

[43] We have provided a new aerosol perspective by using a global model to track the behavior of aerosols coming from particular regions and from particular sectors.

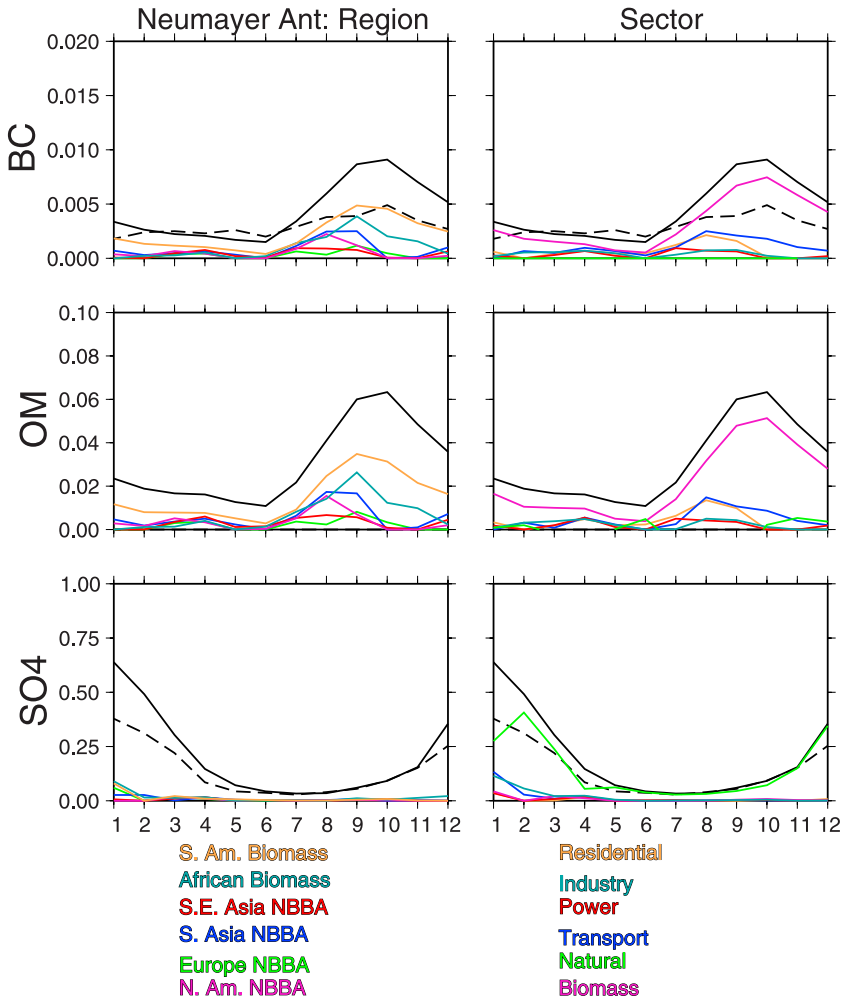

Figure 18. Comparison of model (solid black) and observed (dashed) seasonal concentrations of BC, OM, and sulfate (μg m^{-3}) at Neumayer station, Antarctica. The colored lines show model estimated contributions from various (left) regions and (right) sectors. Sulfate data are for 1983–1995 from *Minikin et al.* [1998], and BC data ares for 1995–2004 from R. Weller (personal communication, June 2005).

This view provides information on consequences of changing aerosol emissions from such sources. It has revealed that aerosol impacts vary greatly, depending on their source sector and region.

[44] Our sectoral experiments indicate that the large negative forcing over midlatitudes of the Northern Hemisphere comes mostly from power and industry sector sulfate. All the large NBBA source regions contribute significantly to these sectors. The sectors with net positive forcing are residential and transport. The transport sector is also an important aerosol source in all NBBA regions. However the residential sector is weighted more toward Asia, where carbonaceous aerosol emissions are especially large.

[45] In addition to such regional sectoral differences, the fate of the aerosols is influenced by regional differences in meteorology and chemistry. For example, the model indicates that Europe and Southeast Asia lack sufficient oxidants to accommodate their SO_2 emissions, so that these regions generate much less sulfate than expected from their SO_2. One implication is that reductions of SO_2 emissions in these regions would not have a proportional impact on sulfate production. Regions which loft aerosols high into the troposphere generally transport their aerosols further. However although both South American and African biomass burning aerosols are lofted, those from Africa are scavenged more efficiently. As a result, South American biomass burning aerosols dominate in much of the Southern Hemisphere. An implication is that reductions of South American biomass burning would have a greater impact on aerosol levels across the Southern Hemisphere than reductions in African biomass burning. Indeed while the model indicates, not surprisingly, that aerosols near source regions are primarily derived from local sources, it also indicates a surprising amount of export out of many of the source regions.

[46] Our model experiments follow up on *Koch and Hansen* [2005] to show that Southeast Asia (including China) contributes the largest portion of Arctic BC; contributions from south Asia (including India) are minimal. Most Arctic BC is from the residential sector, with secondary contributions from biomass burning and the transport and industrial sectors. Organic matter in the Arctic comes mostly from biomass burning in Siberia and the Pacific

northwest. The model indicates that sulfate is the largest component of Arctic haze and is derived mostly from Europe and Southeast Asia; sectoral sources are primarily industry and power.

[47] However, since our model also significantly underestimates carbonaceous aerosol concentrations in Southeast Asia and in Europe, both regions probably actually contribute more to the global BC load. In Southeast Asia other model studies have also reported model underestimations of carbon material. The model of *Park et al.* [2005] underestimated BC by about 60% off the coast of Asia, compared with observations from TRACE-P; they attribute their bias to insufficient emissions. *Kasibhatla et al.* [2002] found a similar underestimate of Asian CO emissions (from fossil fuel and biofuel) compared with observations. Since the residential sector is an important source of both BC and OM in Asia, we may speculate that these sources are underestimated. Note that a larger Asian residential source would increase positive forcing in the Arctic. Clearly more carbonaceous aerosol data, both of emissions and air concentrations are needed in this source region.

[48] In Europe, model sulfate production agrees with observations while carbonaceous aerosols are underestimated, so that net radiative forcing over Europe should be more positive than indicated by the model. Larger residential emissions in Europe would again improve both the OM and BC biases without significantly increasing sulfate. We note however that the European sulfur emissions used here (from EDGAR) are about double those of other estimates (such as those from IIASA [*Koch et al.*, 2006]). Our model agreement with observations appears to be better if we use the EDGAR emissions. A smaller emission inventory would have also contributed to a more positive forcing from Europe; it would also result in smaller European sulfate contribution to Arctic haze.

[49] Although the model underestimates carbonaceous aerosols in Asia and Europe, it was more successful in the United States. Model OM was especially successful in the central and western U.S., where the OM is derived primarily from natural and biomass burning sources.

[50] Over the Atlantic ocean, most of the sulfate pollution originates from North America (10–30% of total sulfate) with secondary contributions from southeast Asia (10–20%) (Figure 9). However, as also discussed by *Koch and Hansen* [2005], most black carbon in the column (mostly above the boundary layer) over the Atlantic comes from Southeast Asia (20–40%) with lesser amounts from North America (20–30%) (Figure 7). Organic material there comes mostly from biomass burning, residential sources and natural emissions (Figure 11). Similar to observations in the TARFOX campaign [*Novakov et al.*, 1997], model carbonaceous mass fraction increases with altitude. Model carbonaceous aerosol concentrations also increase with altitude, and this increase is due primarily to carbonaceous aerosol from Asia that is transported above the boundary layer.

[51] In our experiments we assumed our aerosols to be externally mixed. Particles away from industrial source regions are frequently observed to be internally mixed [e.g., *Clarke et al.*, 2004]. We may speculate about how our results would change if we included internal mixing. Instead of assuming a fixed aging rate, as we have, carbonaceous aerosol solubility might be largely determined by sulfate coating. Such coated particles also have somewhat enhanced absorption [e.g., *Bond and Bergstrom*, 2006]. Thus regions such as Europe and North America, which emit large SO_2 relative to BC would probably be associated with a lessened burden of BC due to enhanced scavenging. This decrease would partially offset the increase in absorption associated with mixing, although it is unlikely that the two effects would cancel. Note however that including internal mixing would introduce nonlinearities to our method of eliminating individual source regions or types. For example, eliminating the power sector would take away a large source of SO_2 that would otherwise have been available to coat BC from the transport sector.

[52] We have used our model experiments to determine the degree to which aerosol forcing can be inferred from emissions. We have found that sulfate cannot be accurately inferred from SO_2 emissions because of oxidant limitation, especially in industrial and power sectors, and coming from Europe and Southeast Asia. The carbonaceous aerosol NBBA forcings are approximately proportional to emissions on a global basis. However this linearity breaks down if we consider specific regions. For example, south Asia's forcings are about double what we expect from emissions. Biomass burning aerosol forcings are poorly related to emissions estimates. In some cases, this can be related to regional effects, such as the relatively long lifetime of South American biomass burning aerosols.

[53] Future studies should address the impacts of subsectors, including particular fuels and/or technologies that have large absorptive emissions. In addition, we plan to investigate how regional and sectoral impacts evolve for historic and future emission scenarios.

[54] **Acknowledgments.** We gratefully acknowledge the IMPROVE network data (vista.cira.colostate.edu/IMPROVE); we also thank Rolf Weller for provision of Antarctic BC data at Neumayer station. Support for this research is from the NASA Radiation Science Program and from the NASA Climate Modeling Program.

References

Albrecht, B. (1989), Aerosols, cloud microphysics and fractional cloudiness, *Science*, *245*, 1227–1230.

Andreae, M. O. (1995), Climatic effects of changing atmospheric aerosol levels, in *World Survey of Climatology*, vol. 16, *Future Climates of the World*, edited by A. Henderson-Sellers, pp. 341–392, Elsevier, New York.

Andreae, M. O., and P. Merlet (2001), Emission of trace gases and aerosols from biomass burning, *Global Biogeochem. Cycles*, *15*, 955–966.

Bell, N., D. Koch, and D. T. Shindell (2005), Impacts of chemistry-aerosol coupling on tropospheric ozone and sulfate simulations in a general circulation model, *J. Geophys. Res.*, *110*, D14305, doi:10.1029/2004JD005538.

Berglen, T. F., T. K. Berntsen, I. S. A. Isaksen, and J. K. Sundet (2004), A global model of the coupled sulfur/oxidant chemistry in the troposphere: The sulfur cycle, *J. Geophys. Res.*, *109*, D19310, doi:10.1029/2003JD003948.

Bond, T. C., and R. W. Bergstrom (2006), Light absorption by carbonaceous particles: An investigative review, *Aerosol Sci. Technol.*, *40*, 27–67.

Bond, T., and H. Sun (2005), Can reducing black carbon emissions counteract global warming?, *Environ. Sci. Technol.*, *39*, 5921–5926.

Bond, T. C., D. G. Streets, K. F. Yarber, S. M. Nelson, J.-H. Woo, and Z. Klimont (2004), A technology-based global inventory of black and organic carbon emissions from combustion, *J. Geophys. Res.*, *109*, D14203, doi:10.1029/2003JD003697.

Chung, S. H., and J. H. Seinfeld (2005), Climate response of direct radiative forcing of anthropogenic black carbon, *J. Geophys. Res.*, *110*, D11102, doi:10.1029/2004JD005441.

Clarke, A. D., et al. (2004), Size distributions and mixtures of dust and black carbon aerosol in Asian outflow: Physiochemistry and optical properties, *J. Geophys. Res.*, *109*, D15S09, doi:10.1029/2003JD004378.

Del Genio, A. D., M. S. Yao, W. Kovari, and K. K. Lo (1996), A prognostic cloud water parameterization for general circulation models, *J. Clim.*, *9*, 270–304.

Del Genio, A. D., W. Kovari, M.-S. Yao, and J. Jonas (2005), Cumulus microphysics and climate sensitivity, *J. Clim.*, *18*, 2376–2387, doi:10.1175/JCLI3413.1.

Giglio, L., G. R. van der Werf, J. T. Randerson, G. J. Collatz, and P. Kasibhatla (2006), Global estimation of burned area using MODIS active fire observations, *Atmos. Chem. Phys.*, *6*, 957–974.

Grini, A., G. Myhre, C. S. Zender, and I. S. A. Isaksen (2005), Model simulations of dust sources and transport in the global atmosphere: Effects of soil erodibility and wind speed variability, *J. Geophys. Res.*, *110*, D02205, doi:10.1029/2004JD005037.

Guenther, A., et al. (1995), A global model of natural volatile organic compound emissions, *J. Geophys. Res.*, *100*, 8873–8892.

Hansen, J., and L. Nazarenko (2004), Soot climate forcing via snow and ice albedos, *Proc. Natl. Acad. Sci.*, *101*, 423–428, doi:10.1073/pnas.2237157100.

Hansen, J., M. Sato, and R. Ruedy (1997), Radiative forcing and climate response, *J. Geophys. Res.*, *102*, 6831–6864.

Houghton, J. T., , Y. Ding, D. J. Griggs, M. Nouger, P. J. van der Linden, X. Dai, K. Maskell, and C. A. Johnson (Eds.) (2001), *Climate Change 2001: The Scientific Basis*, 881 pp., Cambridge Univ. Press, New York.

Jacobson, M. Z. (2002), Control of fossil-fuel particulate black carbon and organic matter, possibly the most effective method of slowing global warming, *J. Geophys. Res.*, *107*(D19), 4410, doi:10.1029/2001JD001376.

Kasibhatla, P., A. Arellano, J. A. Logan, P. I. Palmer, and P. Novelli (2002), Top-down estimate of a large source of atmospheric carbon monoxide associated with fuel combustion in Asia, *Geophys. Res. Lett.*, *29*(19), 1900, doi:10.1029/2002GL015581.

Kirchstetter, T. W., T. Novakov, and P. V. Hobbs (2004), Evidence that the spectral dependence of light absorption by aerosols is affected by organic carbon, *J. Geophys. Res.*, *109*, D21208, doi:10.1029/2004JD004999.

Koch, D. (2001), Transport and direct radiative forcing of carbonaceous and sulfate aerosols in the GISS GCM, *J. Geophys. Res.*, *106*, 20,311–20,332.

Koch, D., and J. Hansen (2005), Distant origins of Arctic black carbon: A Goddard Institute for Space Studies ModelE experiment, *J. Geophys. Res.*, *110*, D04204, doi:10.1029/2004JD005296.

Koch, D., D. Jacob, I. Tegen, D. Rind, and M. Chin (1999), Tropospheric sulfur simulation and sulfate direct radiative forcing in the Goddard Institute for Space Studies general circulation model, *J. Geophys. Res.*, *104*, 23,799–23,822.

Koch, D., G. A. Schmidt, and C. V. Field (2006), Sulfur, sea salt, and radionuclide aerosols in GISS ModelE, *J. Geophys. Res.*, *111*, D06206, doi:10.1029/2004JD005550.

Liousse, C., J. E. Penner, C. Chuang, J. J. Walton, H. Eddleman, and H. Cachier (1996), A global three-dimensional model study of carbonaceous aerosols, *J. Geophys. Res.*, *101*, 19,411–19,432.

Lohmann, U., and J. Feichter (2005), Global indirect aerosol effects: A review, *Atmos. Chem. Phys.*, *5*, 715–737.

Miller, R. L., et al. (2006), Mineral dust aerosols in the NASA Goddard Institute for Space Sciences ModelE atmospheric general circulation model, *J. Geophys. Res.*, *111*, D06208, doi:10.1029/2005JD005796.

Minikin, A., M. Legrand, J. Hall, D. Wagenbach, C. Kleefeld, E. Wolff, E. C. Pasteur, and F. Ducroz (1998), Sulfur-containing species (sulfate and methanosulfonate) in coastal Antarctic aerosol and precipitation, *J. Geophys. Res.*, *103*, 10,975–10,990.

Nilsson, B. (1979), Meteorological influence on aerosol extinction in the 0.2–40-μm wavelength range, *Appl. Opt.*, *18*, 3457–3473.

Novakov, T., D. A. Hegg, and P. V. Hobbs (1997), Airborne measurements of carbonaceous aerosols on the east coast of the United States, *J. Geophys. Res.*, *102*, 30,023–30,030.

Novakov, T., S. Menon, T. Kirchstetter, D. Koch, and J. Hansen (2005), Aerosol organic carbon to black carbon ratios: Analysis of published data and implications for climate change, *J. Geophys. Res.*, *110*, D21205, doi:10.1029/2005JD005977.

Nyeki, S., U. Baltensperger, I. Colbeck, D. T. Jost, E. Weingartner, and H. W. Gaggeler (1998), The Jungfraujoch high-alpine research station (3454 m) as a background continental site for the measurement of aerosol parameters, *J. Geophys. Res.*, *103*, 6097–6107.

Park, R. J., et al. (2005), Export efficiency of black carbon aerosol in continental outflow: Global implications, *J. Geophys. Res.*, *110*, D11205, doi:10.1029/2004JD005432.

Rasch, P. J., M. C. Barth, J. T. Kiehl, S. E. Schwartz, and C. M. Benkovitz (2000), A description of the global sulfur cycle and its controlling processes in the National Center for Atmospheric Research Community Climate Model, Version 3, *J. Geophys. Res.*, *105*, 1367–1386.

Reddy, M. S., O. Boucher, N. Bellouin, M. Schulz, Y. Balkanski, J.-L. Dufresne, and M. Pham (2005a), Estimates of global multicomponent aerosol optical depth and direct radiative perturbation in the Laboratoire de Mtorologie Dynamique general circulation model, *J. Geophys. Res.*, *110*, D10S16, doi:10.1029/2004JD004757.

Reddy, M. S., O. Boucher, Y. Balkanski, and M. Schulz (2005b), Aerosol optical depths and direct radiative perturbations by species and source type, *Geophys. Res. Lett.*, *32*, L12803, doi:10.1029/2004GL021743.

Roberts, D. L., and A. Jones (2004), Climate sensitivity to black carbon aerosol from fossil fuel combustion, *J. Geophys. Res.*, *109*, D16202, doi:10.1029/2004JD004676.

Schmidt, G. A., et al. (2006), Present day atmospheric simulations using GISS ModelE: Comparison to in-situ, satellite and reanalysis data, *J. Clim.*, *19*, 153–192, doi:10.1175/JCLI3612.1.

Takemura, T., T. Nakajima, O. Dubovik, B. N. Holben, and S. Kinne (2002), Single-scattering albedo and radiative forcing of various aerosol species with a global three-dimensional model, *J. Clim.*, *15*, 333–352.

Tang, I. N. (1996), Chemical and size effects of hygroscopic aerosols on light scattering coefficients, *J. Geophys. Res.*, *101*, 19,245–19,250.

Tang, I. N., and H. R. Munkelwitz (1991), Simultaneous determination of refractive index and density of an evaporating aqueous solution droplet, *Aerosol Sci. Technol.*, *15*, 201–207.

Tang, I. N., and H. R. Munkelwitz (1994), Water activities, densities, and refractive indices of aqueous sulfates and sodium nitrate droplets of atmospheric importance, *J. Geophys. Res.*, *99*, 18,801–18,808.

Textor, C., et al. (2006), Analysis and quantification of the diversities of aerosol life cycles within AEROCOM, *Atmos. Chem. Phys.*, *6*, 1777–1813.

Twomey, S. (1997), The influence of pollution on the short-wave albedo of clouds, *J. Atmos. Sci.*, *34*, 1149–11527.

Wang, C. (2004), A modeling study on the climate impacts of black carbon aerosols, *J. Geophys. Res.*, *109*, D03106, doi:10.1029/2003JD004084.

van der Werf, G. R., J. T. Randerson, G. J. Collatz, and L. Giglio (2003), Carbon emissions from fires in tropical and subtropical ecosystems, *Global Change Biol.*, *9*, 547–562.

van der Werf, G. R., J. T. Randerson, G. J. Collatz, L. Giglio, P. S. Kasibhatla, A. F. Arellano, S. C. Olsen, and E. S. Kasischke (2004), Continental-scale partitioning of fire emissions during the 1997 to 2001 El Nino/La Nina period, *Science*, *303*, 73–76.

Ye, B., S. Ji, H. Yang, X. Yao, C. K. Chan, S. H. Cadle, T. Chan, and P. A. Mulawa (2003), Concentration and chemical composition of $PM_{2.5}$ in Shanghai for a 1-year period, *Atmos. Environ.*, *37*, 499–510.

T. C. Bond, Department of Civil and Environmental Engineering, University of Illinois, Urbana-Champaign, Urbana, IL 61801, USA.

D. Koch, NASA Goddard Institute for Space Studies, Columbia University, 2880 Broadway, New York, NY 10025, USA. (dkoch@giss.nasa.gov)

D. Streets, Argonne National Laboratory, Argonne, IL 60439, USA.

N. Unger, Rubenstein School of Environment and Natural Resources, University of Vermont, 321 Aiken Center, Burlington, VT 05405, USA.

G. R. van der Werf, Department of Hydrology and Geo-Environmental Sciences, Vrije Universiteit, Amsterdam, Netherlands.